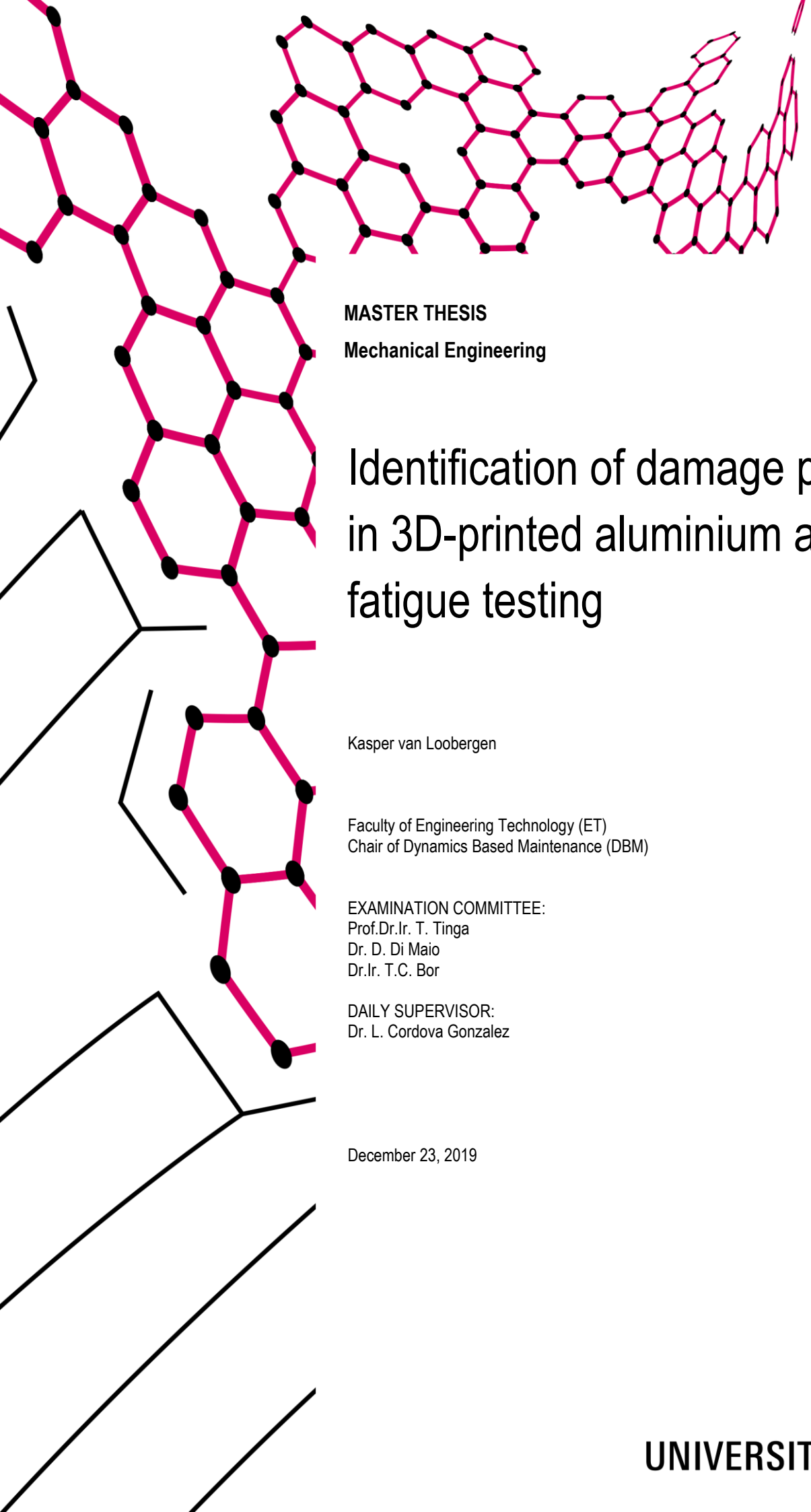

MASTER THESIS

Mechanical Engineering

Identification of damage precursors in 3D-printed aluminium alloy after fatigue testing

Kasper van Loobergen

Faculty of Engineering Technology (ET)
Chair of Dynamics Based Maintenance (DBM)

EXAMINATION COMMITTEE:
Prof.Dr.Ir. T. Tinga
Dr. D. Di Maio
Dr.Ir. T.C. Bor

DAILY SUPERVISOR:
Dr. L. Cordova Gonzalez

December 23, 2019

UNIVERSITY OF TWENTE.

Preface

This work, titled *Identification of damage precursors in 3D-printed aluminium alloy after fatigue testing* was written as part of a graduation assignment for attaining the Masters Degree in Mechanical Engineering at the University of Twente. This thesis describes the process and results of the assignment titled *Characterization of 3D printed material after fatigue testing* at the research chair of Dynamics Based Maintenance (DBM). The work was carried out between April and December 2019.

Laura Cordova was my main supervisor during this assignment. I would like to express my sincere appreciation for all the helpful feedback and assistance that she provided over the entire course of this assignment, she was always available if help was needed. I would also like to thank Tiedo Tinga for the valuable input that he has provided during our regular meetings. Furthermore, the conversations with Dario Di Maio and Ed Habtour were extremely helpful for gathering fresh insights and new points of view regarding the assignment subject. Finally, I would like to thank Nick Helthuis for the time and effort that he has spent to help me with experiments in the Mechanical Testing Laboratory.

Kasper van Loobergen

Enschede, December 2019

Contents

Abstract

Previous research has indicated that damage precursors can be a promising method for predicting and preventing fatigue damage in metal structures. Test plates made from Scalmalloy were 3D-printed using Selective Laser Melting and subjected to fatigue experiments in order to detect damage precursors based on dynamic properties. In this work, the physical properties of these plates that were subjected to fatigue loading are analysed in order to find the cause of change in dynamic behaviour. A series of test plates made from conventionally produced Al 7075-T6 were used as a reference.

A number of approaches to define damage precursors are discussed in this work. Material characterization tests were carried out to help understanding the link between change in dynamic behaviour and physical material changes, as this is essential for properly understanding dynamic damage precursors. Methods that were used to analyse physical properties of the test plates include optical microscopy, confocal microscopy, density analysis, CT-scanning, micro- and nano-indentation and EBSD-analysis. The main cause of the previously observed change in dynamic behaviour can be traced back to early stages of fatigue crack growth, but the applied analysis methods did not indicate significant change of material properties before the first fatigue cracks started to appear.

Also, some attention is given on how damage precursors could be implemented to improve maintenance policies and increase reliability of systems, and what the limitations of damage precursors are in practical applications.

Keywords: Damage precursors, Scalmalloy, SLM, 3D-printing, metal fatigue.

1 Introduction

Additive manufacturing is a promising production method for a wide variety of advanced mechanical components. Thanks to the great amount of shape freedom additive manufacturing technologies allow, it is often possible to replace complex conventionally produced assemblies with one single component that is made by additive manufacturing. Another major advantage of additive manufacturing is the flexibility to change a design without the need to make new forming tools, which is especially advantageous for rapid prototyping purposes or speciality products that are produced in small quantities.

For conventionally produced components, the fatigue behaviour is quite well understood, so it can be accounted for in design and maintenance specifications. For materials that are produced by additive manufacturing, the fatigue behaviour is not understood as thoroughly. Mechanical testing has given some insight in the fatigue behaviour, but macroscopic fatigue properties have not clearly been linked to behaviour on the microscopic level of the material. If changes in a material that precede damage ('damage precursors') are better understood, it could help to detect upcoming failures well in time or aid to predict remaining component life more accurately. Being able to understand and detect damage precursors could lead to increased system reliability and reduction of overall operation costs.

Prior to the current research, fatigue testing has been performed on test plates made from an aluminium-magnesium-scandium alloy (Scalmalloy) using Selective Laser Melting (SLM), an additive manufacturing process for metals. Since these samples have been subjected to different, well-documented sequences of fatigue loading, they are very suitable for use in the current research. Previous studies have suggested that changes in dynamic response can be used as a damage precursor [1] [2]. However, the link between changing dynamic properties and microstructural changes is not yet fully understood. This report aims to find this relation by analysing the test plates after they have been subjected to fatigue testing. If the link between fatigue behaviour and microstructure is better understood, parameters of the production process can be optimized. If it is known how damage precursors on the microstructural level can be detected, it may become possible to replace components that are affected by fatigue before actual failure occurs without having to reduce the useful component life with early preventive replacement.

2 | Research outline

This chapter will give the problem statement of this report, and define the research questions that should be answered in order to fulfil the research objectives. At the end of the chapter, a description of the research approach and the outline of this report are given.

2.1 Problem statement

The main focus in this work centred around the concept of damage precursors to predict and prevent fatigue damage in aluminium components that are produced using additive manufacturing. The concepts of metal fatigue, additive manufacturing and damage precursors are described briefly in this section, to gather more insight in the relevance of the problem that is studied in this work.

2.1.1 Metal fatigue

Over the past decades, a large amount of research has been performed in the fields of fatigue behaviour and micro-structure of metals. Fatigue in materials is gradual weakening of material when it is subjected to repeated loads. The Amount of fatigue cycles that a component can endure depends on a number of variables, such as the material that it is made from, the load that is applied and the amount of load cycles that the component is subjected to. Metal fatigue initially starts with the formation of microscopic cracks that slowly grow larger as the component is subjected to more load cycles. Eventually, the structure is weakened to a point where it can no longer cope with the applied load. At that point, a sudden failure occurs. Figure 2.1 shows a typical example of full fatigue failure, where the dark area indicates the area of initial fatigue crack growth and the lighter area is where sudden brittle fracture has occurred.

Figure 2.1: Example of fatigue failure in conventionally produced aluminium [3].

2.1.2 Additive manufacturing

The field of additive manufacturing (AM), more commonly known as '3D-printing', has been extensively researched since the 1980's [4]. Additive manufacturing is a term that is used for several significantly different production processes, which all have in common that material is added in several small steps until the finished product is obtained, opposed to conventional 'subtractive manufacturing' methods such as milling and lathing, where material is gradually removed from a blank in order to produce a finished part. Depending on the additive manufacturing method that is applied, a wide variety of materials, including plastics, metals and ceramics can be processed [4].

A significant growth of interest in AM of metals can be seen over the past decade as the technologies have been maturing. However, the link between microstructure and fatigue behaviour of additively manufactured metals is rather unknown, which makes it difficult to make accurate estimations of expected lifespan for additively manufactured components.

2.1.3 Damage precursors

The concept of damage precursors refers to find changes in material behaviour and properties that occur before detectable fatigue damage starts developing. The two most promising applications of damage precursors are improvement of maintenance processes and increase of system reliability.

Once a damage precursor has been detected in a component, replacement parts can be ordered and maintenance can be scheduled to replace the component before failure occurs. By predicting replacement via damage precursors, the required stock of spare components can be reduced, decreasing costs that are involved with stocking spares. If a type of damage precursors is chosen that can be observed during normal operation, intervals of regular inspections can be extended to further reduce costs. If a suitable damage precursor is used, it is also possible to extend the interval for preventive replacement to avoid unnecessary replacement of components. All these factors contribute to optimization of maintenance procedures, and could reduce overall operation costs in industrial applications.

Besides reducing maintenance costs, damage precursors can also be used to increase reliability of a system. In many applications, there is a balance between the desired reliability and the maintenance costs that are necessary to keep the reliability at this desired level. By knowing suitable damage precursors for critical components, replacement can be scheduled before failure occurs, thus improving reliability of the system.

2.2 Research objectives

The overall objective of the research in this report, is to gather understanding in how additively manufactured aluminium alloys change before fatigue cracks start developing, and to link this with previously observed dynamic behaviour. These changes can be referred to as 'damage precursors', and they may be a useful tool for improving reliability and maintenance policies. The following three research questions are formulated in order to fulfil the research objectives:

- What different approaches are possible to define damage precursors?
- How do the microstructure and physical properties of SLM-produced Scalmalloy change before fatigue failure occurs?
- How can the damage precursors be implemented to optimize maintenance policies?

2.3 Research approach and report outline

The approach to find the answers to the research questions is based on a series of test specimens that have undergone vibration fatigue tests as part of previously performed research. A major part of the report will be dedicated to experiments that were performed in order to evaluate the properties of these test specimens before and after fatigue testing.

The report will start with an investigation about how a damage precursor can be defined in chapter 3, which is meant as a general introduction in the concept of damage precursors. Some different insights in how the concept of damage precursors can be approached in this chapter as well. Chapter 4 gives a description of the relevant production process and the considered materials. It also describes the available samples and the analysis methods that will be used to characterize the microstructure. The results are presented in chapter 5, followed by a discussion of the results in chapter 6. Chapter 7 contains the conclusions and recommendations.

3 | Definition of damage precursors

The objectives of this research are centred around the concept of 'damage precursors'. There is no universal definition of what a damage precursor is, but it generally refers to a change in a material or structure that occurs shortly before actual damage develops. However, there is no unambiguous definition of what damage is, and consequently, there is no clear definition for damage precursors either. In this chapter, several approaches for defining damage and damage precursors are proposed. It depends on the specific application which of these approaches is the most suitable.

3.1 How to define damage

To define an appropriate damage precursor, there must first be a clear definition of damage. There are many possible ways to define damage, so it is important to use a definition that is as relevant as possible. Firstly, all definitions of damage that are described in literature can be divided in cosmetic damage and structural damage. Since cosmetic damage has only impact on the appearance of a component but not on the functionality, it is not useful to consider any form of cosmetic damage for the application of damage precursors.

Even if definitions that only regard cosmetic damage are discarded, there are many different ways to define structural damage. The most accurate for this report is 'changes introduced into a system that adversely affect its current or future performance' [5]. This definition is suitable for cases where the current performance of a system is affected, since performance degradation is generally relatively easy to detect.

For changes that only affect performance in the future, it is more difficult to define which changes should be considered as damage. Firstly, it depends on which parameters are used to measure performance. In situations where stiffness of a component is critical for the performance of a system, a minor drop in stiffness is already considered as a performance degradation, but there are also many applications where a drop in stiffness of a component has no influence on the performance. The same holds for reliability, since it is sometimes possible to actively monitor this as a performance parameter, but there are also many situations where this is not done.

It is also possible to consider microscopic cracks as damage, even if they do not yet affect performance, since most cracks will generally grow gradually until performance degradation or failure occurs. If the behaviour of a material before the occurrence of fatigue cracks is known, it is also possible to consider a change in physical properties of material that is known to precede cracking as damage. Situations where changes are present without affecting performance are of particular interest when considering damage precursors, since the difference between damage precursors and early stages of damage is often a grey area.

Summarizing, 'changes introduced into a system that adversely affect its current or future performance' is a suitable general definition for damage, but it is essential to set component-specific thresholds to make a clear distinction between damage and a damage precursor.

3.2 Properties of a suitable damage precursor

When it is clear how damage can be defined for a certain situation, the next step is to find out how damage precursors can be defined. This section describes the properties which a suitable damage precursor should comply to in order to enable us to evaluate the suitability of different definitions that will be described later on.

3.2.1 Ease of precursor detection

To make sure that a damage precursor is practically usable, it must be possible to detect the precursor without excessive effort. If a component must be removed from the system that it is part of, the removal of this component will probably cause downtime and labour costs. If a very complex and expensive procedure is needed for detection of a damage precursor, it is likely that preventive replacement is less expensive than the procedure to check whether a damage precursor is present. The same holds for situations where excessively expensive monitoring equipment is required for detection of a damage precursor, so in those situations it will not be economical to use such a damage precursor.

3.2.2 Time of precursor development in relation to component life

A good damage precursor should be detectable at a suitable point in the life of a component. Obviously, this should be before directly detectable damage develops. However, it is unfavourable if a damage precursor starts developing very early in the component life, because this may trigger preventive replacement long before it is actually necessary, thus reducing the functional life of the component.

The P-F interval that was described by Moubray [6] can be a useful tool for determining whether a damage precursor is suitable. In this model, it is assumed that a system starts to degrade immediately after it is put into use. At some point P, an upcoming failure becomes detectable. Point F is the moment where functional failure occurs. The time between P and F is called the P-F interval. This concept is illustrated in figure 3.1. A suitable damage precursor should ensure a P-F interval that is long enough to ensure timely detection of damage, but the P-F interval must not be too long in order to avoid premature replacement of parts that are still perfectly usable.

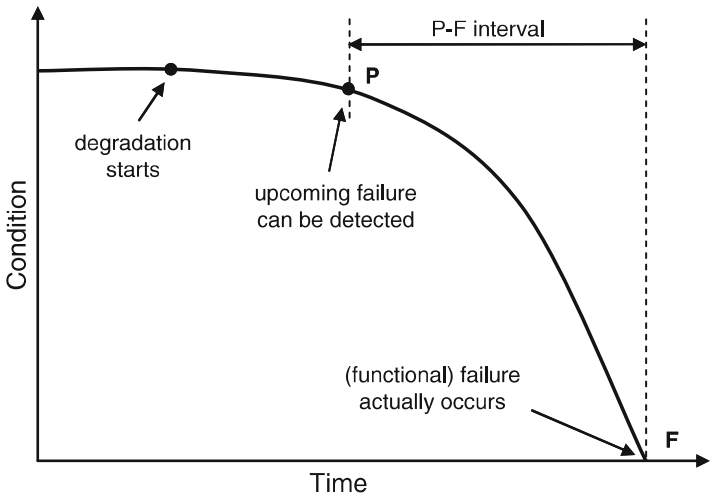

Figure 3.1: Graphical representation of the P-F interval in relation to component life [7].

3.2.3 Distinction between damage and damage precursor

It may seem obvious, but it is very important to make a clear distinction between a damage precursor and actual damage. In many cases, some observation that is qualified as a damage precursor, can also be regarded as an early stage of damage development. Therefore, it is important to know the degradation and failure behaviour of a component, and to define what the distinction between a damage precursor and actual damage is.

3.2.4 Consistence in occurrence of precursor

In order to rely on damage precursors for the maintenance policy of a component in a system, it is important that a damage precursor always develops before actual damage occurs, so false positive and false negative errors are avoided. A false positive error is when a damage precursor is detected without any imminent damage, and a false negative is when damage occurs without the precursor showing up in advance [8]. Both situations are highly undesirable, so if the precursor only develops in a limited number of situations, it can no longer be relied on as a means of maintenance optimization.

3.3 Possible damage precursors

Similarly to the different possible definitions of damage, there are also several approaches possible for the definition of damage precursors. The definitions of each precursor are somewhat linked to the definitions of damage, but some of the proposed damage definitions can be linked to more than one definition of damage. The different approaches for a damage precursor are described in this section.

3.3.1 Damage precursor based on dynamic response

One method to define a damage precursor, is to relate it to changes in dynamic response of a structure. Habtour et al. [1] have determined that fatigue can lead to a decrease in stiffness due to a combination of changes that can occur in the material. The change in dynamic response as a result of fatigue was also the subject of the master's thesis of Dragman [2], who suggested that the decrease in stiffness as a result of progressing fatigue can be displayed in the form of backbone curves, such as depicted in figure 3.2. Both Habtour and Dragman have suggested that changes in dynamic response can be a suitable damage precursor.

In the series of backbone curves that is depicted in figure 3.2, each curve represents the dynamic response of a test specimen that is subjected to a frequency-sweep vibration signal after a certain number of fatigue load cycles. The horizontal axis represents the normalized frequency related to the beam in pristine condition (Ω), and the vertical axis the measured amplitude (α) divided by the length of the beam (L). A gradual decrease in stiffness can be observed when the amount of fatigue cycles increases.

Advantages and drawbacks

Using dynamic response as a method for defining damage precursors has several advantages. If the dynamics of a system in regular operation are well known, it is relatively easy to detect subtle changes in response during regular operation. Especially if a suitable array of sensors can be installed, it might be possible to use dynamic based damage precursors for an on-line condition monitoring application. In situations where stiffness of a component is critical, it is

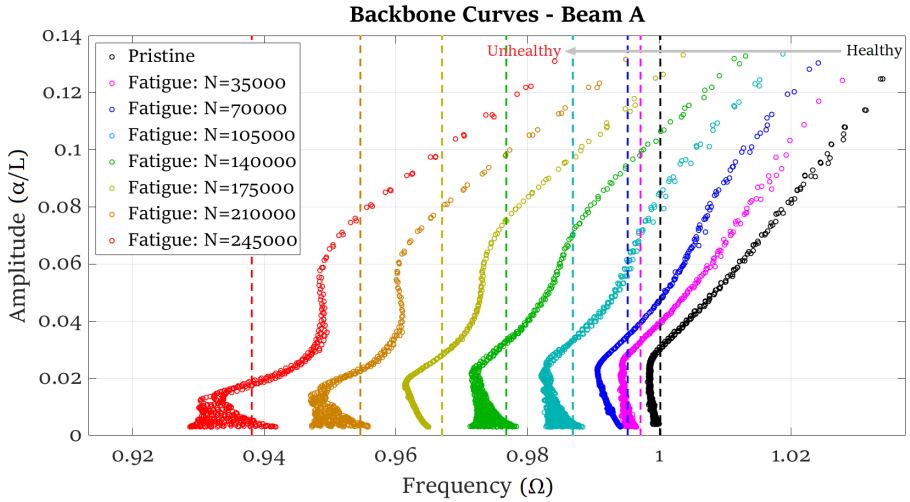

Figure 3.2: Backbone curves showing changes in dynamic response as a result of metal fatigue [2]

also easy to make the distinction between damage and the precursor, since a pre-determined decrease of stiffness can be used as a failure criterion.

There are also some drawbacks for this method. The most fundamental drawback is, that it is not necessarily understood what the underlying cause of a change in dynamic response is. Therefore, it must be very well understood what exact change in dynamic response of the system is caused by a damage precursor. Whether this method is feasible, will depend greatly on the specific application, and the dynamic behaviour upon degradation must be determined for every new application.

The dynamic approach for damage precursors could comply to all criteria that are described in section 3.2, but only if the expected failure behaviour of the component that is considered is well known.

3.3.2 Damage precursor based on physical changes

As an alternative to the dynamics based definition, the physical properties of the material can be used as a criterion for the damage precursor, since a decrease in stiffness will always have an underlying cause that can be traced back to a change in properties of the material. It is possible that changing properties can be detected before a change in stiffness can be observed.

Examples of properties that can be used as damage precursors in this method, are changes in surface roughness, mechanical properties such as hardness and elastic modulus or a change in crystal structure of the material. It is also possible that microscopic cracks are present that are invisible when using regular optical methods, an can thus be considered as damage precursors if more accurate analysis methods are utilised.

Advantages and drawbacks

An advantage of this method compared to the dynamic approach is that it uses the root cause of the change in dynamics as definition of damage precursor. A local change in physical properties is easier to localise than a general change in dynamic response, so it may be easier to pinpoint the root of damage. Therefore, this approach may be useful to gather a better

understanding in how and why a dynamics based damage precursor develops.

Drawbacks of this method are that microstructural changes are generally hard to detect and require advanced analysis equipment. This makes it likely that detecting damage precursors in this manner is too time consuming for most practical applications, especially if a component is integrated into a system. That makes this approach only feasible if it is well known which changes signal a damage precursor and how to look for them. Another limitation is that destructive analysis methods cannot be used if it is desired to keep a component in use if no damage precursors are found.

To verify whether this approach is capable of fulfilling all criteria from section 3.2, more research is needed in order to understand the development of material changes as the material ages. It is also likely that a method that works well for some material, will not be suitable for a different material, so it is highly component-dependent.

3.3.3 Damage precursor based on reliability

A third way to define damage precursors, is to make a connection with the concept of reliability. Since reliability is clearly defined in literature, it can be used as a basis for defining damage and damage precursors.

To obtain a suitable definition of a damage precursor based on reliability, some definitions must be clarified. Reliability and failure are clearly defined by literature. Tinga [7] describes failure as 'reaching such a state that the intended function of the part or system can no longer be fulfilled'. Reliability is defined as the statistical probability that failure will not occur during a certain period of operation.

To define this approach of a damage precursor, the operational lifespan of a component is divided into two periods: a period where the reliability meets the set requirements by the operator, followed by a period where the reliability of the component has dropped below the required minimum. If the component is kept in operation, it will eventually fail. This concept is depicted schematically in table 3.1.

New	Reliability meets requirements		Reliability insufficient ('Damaged')	Failure
		Precursor stage		
Operation time →				

Table 3.1: Schematic representation of component lifespan

During the period where a component meets reliability requirements, it is considered to be 'healthy'. After the reliability drops below the minimum requirement, it is considered to be 'damaged'. This distinction between healthy and damaged enables us to define the 'precursor stage', near the end of the healthy stage. The component is still functioning within reliability requirements during the precursor stage, so it is not considered to be damaged.

The challenge for defining a suitable damage precursor is to find a change in the component that occurs before the component is considered 'damaged', but that is observable early in the 'precursor stage' The desired duration of the precursor stage depends on a number of factors, including but not limited to inspection intervals and lead time for replacement.

Advantages and drawbacks

A drawback of this method is that reliability is a statistical parameter. Therefore, a definition of damage based on reliability is only usable if a relatively large number of components is

in operation. If this method is applied to a component that is widely used, it can provide a statistical solution for the problem of distinguishing damage from damage precursors. A constraint for this to work is, that a suitable change in properties can be found during the 'precursor stage'.

To see whether this approach complies to the requirements that were set in section 3.2, it would be useful to apply it to a system where sufficient failure statistics are available. However, this is outside the scope of this work.

3.4 Suitability of approaches

Three different approaches of defining a damage precursor were presented in this chapter. It depends on the specific application which of these is the most suitable. All approaches have different advantages and drawbacks, and depending on the application and the goal with which damage precursors are used, the most suitable can be chosen. It may also be possible to use a combination of different approaches to obtain optimal results.

It must be noted that all three components can be related to each other, because change in dynamic properties is most likely a result of microstructural degradation, and this degradation also leads to decreased reliability as a component ages. Linking the tree proposed methods can therefore be a suitable method to gather more understanding about how a component ages during its operational lifespan.

The remainder of this report will mainly focus on finding the relation between the dynamic and physical precursors. The aim is to find what physical properties change at the point where previous research has found development of a dynamic damage precursor.

4 Methods and materials

In this chapter, a description will be given of the used additive manufacturing method and aluminium alloy, followed by a summary of possible material characteristics that may be relevant to analyse when searching for damage precursors. A summary is given of the samples that are available from previous fatigue experiments, and the methods that will be used to analyse the samples are described, including the required preparation steps.

4.1 The SLM process

This report focusses on samples produced by the Selective Laser Melting (SLM) process, which is an AM-method that belongs to the powder bed fusion (PBF) category and can be used for the processing of a variety of metals in powder form. Especially alloys that are suitable for welding, such as certain stainless steels, titanium alloys and some aluminium alloys are suitable for usage in the SLM process.

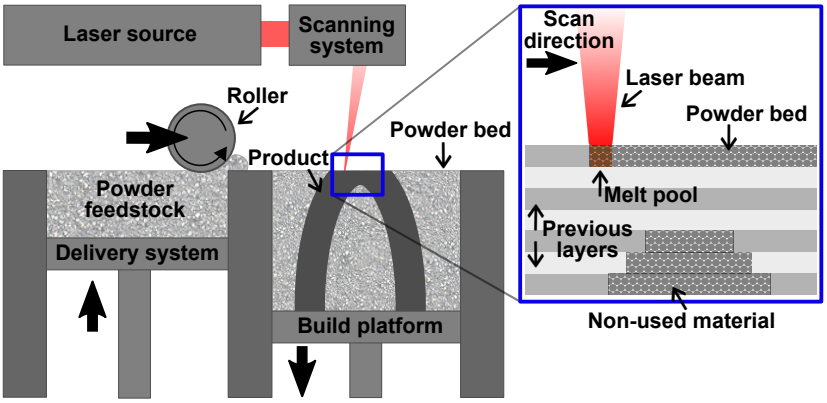

Figure 4.1: Schematic representation of the SLM process [9].

The SLM process makes use of a powerful laser to melt metal powder in order to create three-dimensional metal objects layer-by-layer. A schematic representation of the process is displayed in figure 4.1. The process starts with a single layer of powder that is deposited evenly on the bottom of a build chamber. The laser traces over this layer of powder in order to melt and fuse the regions that belong to the finished product. After the laser has finished a layer, the bottom of the build chamber is moved down one layer thickness. A new layer is deposited on top of the old layer, generally by a counter-rotating roller, and the laser starts fusing the next layer. These steps are repeated until the entire product is finished. Afterwards, the residual powder can be removed from the build chamber and the final part remains [10], [11]. There are several different parameters that influence the properties and quality of the finished product. These parameters include laser power-density, laser tracing speed, temperature of the build chamber, layer thickness, properties of the printed material and powder quality.

4.2 Properties of considered alloys

Since this work mainly focusses on the behaviour of Scalmalloy, it is interesting to get an insight in the relevant properties of this material. Scalmalloy is the brand name that is used for an aluminium alloy that was developed especially for powder bed fusion manufacturing by ApWorks, a daughter company of Airbus. The properties of Scalmalloy are compared to conventionally produced (extruded) Al7075-T6, because specimens made from this material are available as a reference.

4.2.1 Mechanical properties

ApWorks has specified several material properties of Scalmalloy [12] that are obtained in Scalmalloy when optimal printing conditions are applied and the proper age hardening process is carried out after printing. Test plates made from conventionally produced Al 7075-T6 has mechanical properties that are very similar to Scalmalloy. The most important mechanical properties for both Scalmalloy and Al 7075-T6 are listed in table 4.1. The T6 designation for Al 7075 describes a solution heat-treatment process, followed by artificial ageing that greatly improves mechanical properties such as yield strength, tensile strength and hardness [13].

Material Property	**Scalmalloy**	**Al 7075-T6**
Young's modulus	70 GPa	$69 - 76$ GPa
Yield Strength	470 MPa	$359 - 530$ MPa
Tensile strength	520 MPa	$434 - 580$ MPa
Elongation at break	13%	$2 - 10\%$
Vickers Hardness	180 HV0.3	$152 - 168$ HV
Density	2.67 g/cm^3	$2.77 - 2.83$ g/cm^3

Table 4.1: Mechanical properties of Scalmalloy [12] and Al 7075-T6 [13].

4.2.2 Composition

Although Scalmalloy and Al 7075-T6 have similar mechanical properties, they have quite a different composition. The main alloying element in Scalmalloy is magnesium. In general, Al-Mg alloys are known for their good weldability, which also makes them suitable for additive manufacturing. The addition of small amounts of scandium and zirconium in Scalmalloy enables formation of Al_3(Sc,Zr) precipitates, which significantly improves the mechanical properties of the alloy [14]. The composition of Scalmalloy is listed in table 4.2

Element	Al	Mg	Sc	Zr	Mn	Si	Fe	Zn	Cu	Ti	O	V
wt% (min)	91.6	4.00	.60	.20	.30	.00	.00	.00	.00	.00	.00	.00
wt% (max)	94.9	4.90	.80	.50	.80	.40	.40	.25	.10	.15	.05	.05

Table 4.2: Composition of Scalmalloy [15].

Even though the mechanical properties of Scalmalloy and Al 7075-T6 are similar, the compositions are quite different. Both alloys contain mainly aluminium, but the main alloying element is Al 7075 is zinc and the magnesium percentage is significantly lower compared to Scalmalloy, and no scandium is present in Al 7075. The composition of Al 7075 is shown in table 4.3.

Element	Al	Zn	Mg	Cu	Cr	Fe	Si	Mn	Ti
wt% (min)	87.2	5.1	2.1	1.2	.18	.00	.00	.00	.00
wt% (max)	91.4	6.1	2.9	2.0	.28	.5	.40	.3	.2

Table 4.3: Composition of Al 7075 [13].

The processibility of Scalmalloy and Al 7075 is also very different. Scalmalloy is very suitable for welding, a property that is shared between most alloys that are suitable for additive manufacturing. On the other hand, AL 7075 is unsuitable for welding, and mainly suitable for hot forming processes. If it is highly desired to process Al7075 with SLM, it was found by Montero-Sistiga et al. [16] that addition of $\sim$ 4% silicon can improve the SLM-processibility of Al7075. Aluminium alloys from the 5000-series, that are similar in composition to Scalmalloy, are more usable for cold forming and press forming methods, and also suitable for welding [13].

4.2.3 Crystal structure

The grain structure of Scalmalloy generally consists of two different regions, as shown in figure 4.2 [14]. There are regions with rather large grains that are relatively long in the build direction, and regions with very fine, equiaxed grains. The reason for these two distinct grain types originates from the difference in cooling rate within a melt-pool and re-heating that occurs in some regions during the printing process. This behaviour is not present in conventionally produced alloys, where the grain size distribution is much more uniform.

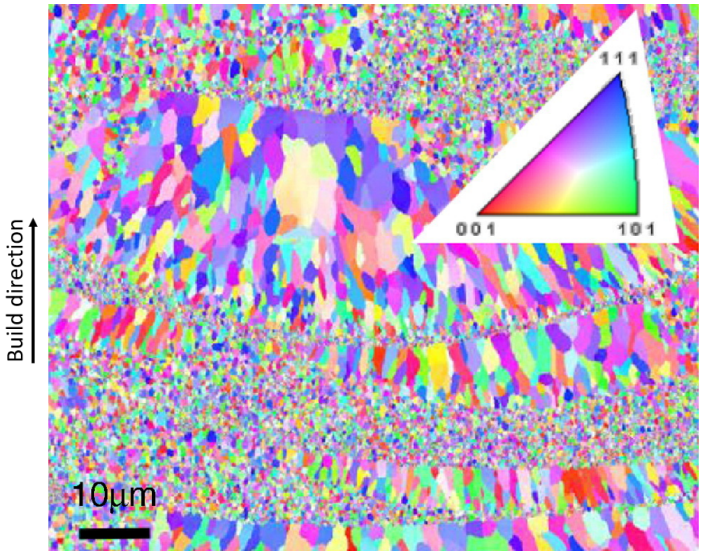

Figure 4.2: Typical grain structure present in Scalmalloy [14]

4.2.4 Porosity and its relation to moisture

Due to the large total surface area of the metal powder that is used in additive manufacturing, it tends to attract moisture. Presence of moisture in the metal powder will lead to the formation of hydrogen pores when the powder is melted during the printing process [17]. These pores will affect the integrity of the material and can form initiation points for metal fatigue. For aluminium powders, it has also been shown that the flowability of powder

decreases if the moist content is high, which could make it difficult to spread a uniform layer of powder on top of the build chamber [18]. If powder has been exposed to excessive moisture, it can be dried by passing over the powder with a low-powered laser beam [17] or by air-drying [19].

When a part is printed using the SLM-method, not all the powder in the build chamber is used. Due to the high cost of metal powders, it is common that the residual powder from the build chamber is re-used. After the original packaging of the metal powder is opened, it will start to collect moisture. This happens because air always contains some water vapour. Therefore, re-used metal powder tends to contain more moisture than virgin powder. Drying powder before re-use has proven to increase the density of printed parts.

There are several different methods to analyse the porosity of a metal part. Wits et al. [20] have made a comparison between several different methods. They found that both measuring the density of a component using Archimedes' principle and optical surface porosity measurements can yield sufficiently accurate results. CT-scanning is also a suitable option, but it is limited to relatively small volumes of material. A benefit of CT-scanning over the other two options is that it can give insight in interconnectivity between pores.

4.3 Previous vibration experiments

The current research is performed as a follow-up of previous vibration fatigue experiments. In these experiments, the dynamic response of aluminium test specimens was monitored during vibration fatigue experiments. To this end, the beams were clamped between two steel blocks and vibrated transversely. The excitation of the beams was measured by a laser vibrometer during the experiments. A control system ensured that the beams were vibrated in their eigenfrequency, and this frequency was adjusted continuously during the experiments. An example of the results from these experiments is shown in figure 4.3, where the eigenfrequency of a beam is plotted against the number of vibration cycles.

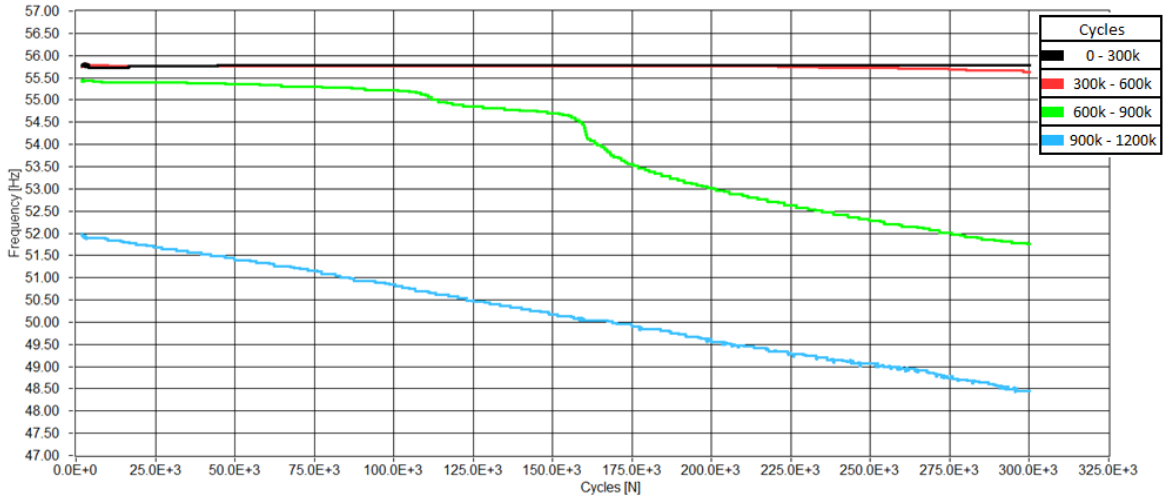

Figure 4.3: Dynamic response of Al7075-T6 during high-cycle fatigue experiment.

The results in figure 4.3 show a very stable response up to 700,000 cycles, whereafter the eigenfrequency starts to drop. Especially around 775,000 cycles, a very steep drop is observed, followed by a linear decrease of eigenfrequency until the end of the experiment around 1,200,000 cycles. This could be explained by formation of a fatigue crack that starts around 700,000 cycles, and gradually grows, thus causing a decrease in stiffness of the beam.

However, these dynamic results were not verified by analysis of material changes in the specimens after or during the vibration experiments, so one of the aims for this research is to investigate what kind of change is present in the material when the eigenfrequency of the beams starts to drop.

4.4 Available materials

There are four different sets of specimens that are available after the dynamic fatigue experiments. Three of these sets are made by SLM from Scalmalloy that received a precipitation hardening procedure after production. One of the Scalmalloy sets was made from powder that has never been used before ('virgin'), one from powder that was used 4 times before, and one from powder that was used 5 times and dried prior to production of the test plates. The fourth set is made from conventionally produced Al 7075 that was heat treated to a T6-state. The material condition of each specimen set is listed in table 4.4.

Sample nr.	Material	No. of samples
6901	Scalmalloy (4x re-used, not dried)	4
6902	Scalmalloy (virgin)	4
6903	Scalmalloy (5x re-used, dried)	4
1001 - 1006	Al 7075-T6	6

Table 4.4: Materials of specimens

All test specimens are flat plates with a length of $150mm$, width of $50mm$ and a thickness of $1.0mm$. The freely vibrating portion of the plates while clamped during fatigue testing had a length of $120mm$. A set-up that was used for vibration tests is shown in figure 4.4a. After the experiments, the samples could be flipped lengthwise to be used a second time. The two sides of the samples are referred to as the a- and b-side in the remainder of this report.

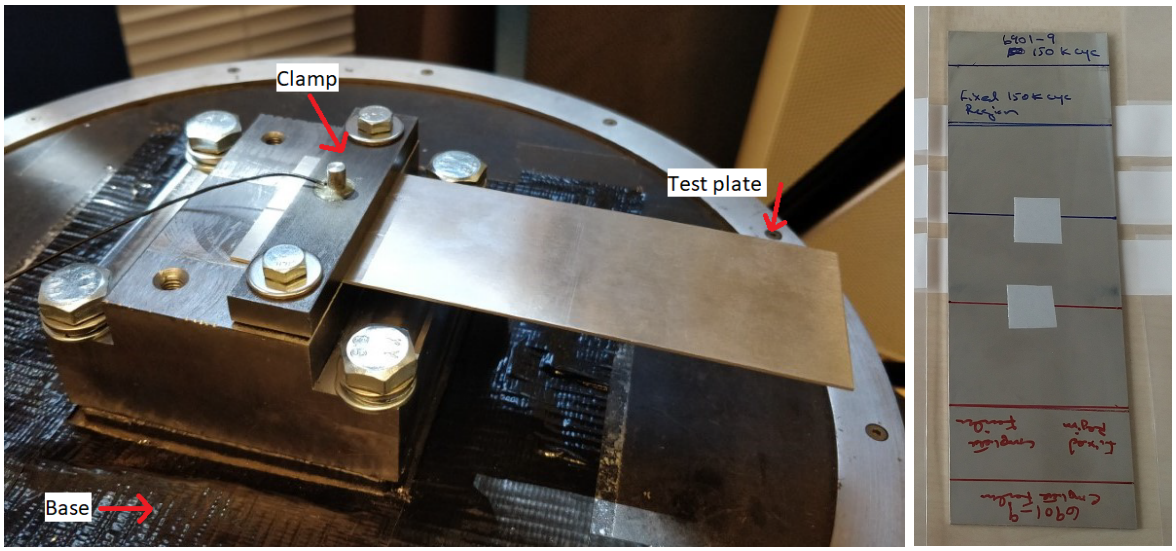

(a) Test set-up (b) Test plate

Figure 4.4: The test set-up for fatigue tests. The base was vibrated in the eigenfrequency of the test plate to apply fatigue load.

The a-side of each sample was clamped and vibrated until fatigue cracking started to appear. The b-side of most samples was clamped and vibrated a pre-determined number of cycles, but not for all. Table 4.5 lists all available samples with the amount of cycles for each side, along with some other remarks. Some specimens were broken in pieces on the a-side for previous analysis, this is mentioned in table 4.5 as well.

Specimen	**Cycles a-side**	**Cycles b-side**	**Remarks**
6901-6	$347,856$	$\sim 75,000$	
6901-8	$340,839$	N/A	
6901-9	$348,191$	$\sim 150,000$	
6901-10	$347,855$	$\sim 300,000$	Slight cracking visible at b-side
6902-1	$263,532$	$\sim 225,000$	Low cycles on a-side due to unbalanced torque, crack at a-side hard to see
6902-3	$399,366$	N/A	
6902-4	$432,750$	$\sim 75,000$	
6902-5	$426,817$	$\sim 150,000$	
6903-1	$400,527$	$\sim 150,000$	
6903-2	$410,721$	$\sim 75,000$	
6903-3	$410,498$	N/A	
6903-5	$426,072$	$\sim 300,000$	Specimen broken at a-side (4 pieces), part of cracked region missing
1001	$1,126,414$	N/A	Crack at a-side hard to see with naked eye
1002	$642,146$	N/A	
1003	$1,154,328$	N/A	
1004	$938,253$	N/A	
1005	$1,375,886$	$\sim 300,000$	Specimen broken at a-side (5 pieces), no missing pieces
1006	$1,200,991$	$\sim 600,000$	Specimen broken at a-side (5 pieces), part of cracked region missing

Table 4.5: Available samples after fatigue testing.

4.5 Selected analysis methods

After the relevant material characteristics of the considered materials were clarified, it was investigated which methods are available to analyse the material characteristics. The chosen analysis methods are described in this section.

4.5.1 Optical analysis

Initially, an optical analysis will be performed. This will be done in two steps: the first step is a simple visual inspection of the samples with the naked eye. The clamping region is particularly interesting, since it is expected that fatigue damage will occur in that region. Special features to look for, are cracks, scores, ridges or other surface defects. It is expected that features down to a size of 0.1mm can be distinguished with the naked eye [21].

After the visual inspection, the clamping regions will be analysed with an optical microscope. To this end, a Keyence VXH-5000 microscope is available that can quickly produce digital images of the surface. Surface features and defects down to a size of 1 μm can be observed with this microscope. Polishing of the samples may reveal details that can be obscured by the surface roughness of the samples in as-receives state. Polishing also makes porosity of the specimen surface visible.

4.5.2 Confocal microscope analysis

Since the optical microscope that is used has no stereoscopic capabilities, another method must be used to map the roughness parameters of the surface. Confocal microscopy makes use of a scanning laser beam that is capable of producing three-dimensional images and can detect features up to nanometer-scale. The high resolution in vertical direction makes it a very useful tool for roughness analysis and the high magnification factor makes is very suitable for detecting features in the microstructure of the specimen.

The microscope that is used for the roughness analysis is a Keyence VK 9700 confocal laser scanning microscope. Particular attention will be given to crack tips, because the confocal microscope might be capable of providing more detail and thus reveal the presence of cracks where they were no longer visible by the optical microscope. Roughness parameters will be identified near fatigue affected areas, as well as far away from the clamp region, in order to find whether roughness parameters will change before fatigue fracture occurs. The roughness analysis using the confocal microscope does not require any specific preparation, apart from cleaning the specimens using isopropyl alcohol.

4.5.3 Archimedes density measurement

Since the porosity analysis using optical microscopy only gives information about porosity on the surface, the Archimedes method can be used additionally to determine the overall porosity within the samples. This method is based on the weight difference of the samples in a liquid compared to the weight in air. If the density of the liquid is known, the density of the sample can be calculated by equation 4.1 [22], with ρ_s the density of the sample, m_1 the weight of the sample in air, m_2 the weight of the material when submerged in liquid, and ρ_{fl} the density of the liquid.

$$\rho_s = \frac{m_1}{m_1 - m_2} * \rho_{fl} \tag{4.1}$$

To make sure that the density measurement is not influenced by the porosity on the surface, the Scalmalloy was sealed with lacquer before the experiment. Equation 4.1 can be expanded to compensate for the application of lacquer. In this situation, m_1 is the weight of the material in air without lacquer, m_3 is the weight of lacquer and m_4 is the weight of the sample (with lacquer) in water.

$$\rho_s = \frac{m_1}{\left(\frac{(m_1+m_3)-m_4}{\rho_{fl}}\right) - \left(\frac{m_3}{\rho_l}\right)} \tag{4.2}$$

Spierings et al. [22] discovered that the Archimedes method can give more reliable data about the porosity of aluminium alloys. By comparing the result of the optical porosity measurement and the Archimedes measurement, it can be verified how these methods compare to each other when analysing SLM-produced material.

4.5.4 CT-scanning

During the course of the research, an opportunity came up to send some samples to an external research institute for CT-scanning. For these scans, the clamp region of one fully fatigued specimen from each batch was cut out and sent away. CT-scanning (Computed Tomography Scanning) makes use of x-ray images to visualize the inside of a structure. To this end, a large number of cross-sectional images is made, that can be combined to form a three-dimensional model of a sample. CT-scanning makes it possible to verify how deep the cracks are that appear on the surface, and to get a better idea about how the fatigue cracks are influenced by porosity in the material. It was also found to be a suitable density analysis method by Wits et al. [20].

4.5.5 Grain structure analysis

There are several different methods to visualize the grain structure of the test samples. The suitability of methods depends on the material that is analysed, and the amount of detail that is desired. Some experiments were performed in order to find the most suitable way to analyse the grain structure of Scalmalloy.

Etching and optical analysis

In most materials, the grain structure can be visualized sufficiently with optical microscopy. This method only works if the specimen is properly prepared. Preparation starts with polishing, in order to obtain a smooth, mirror-like surface. To make the grain boundaries visible on a polished surface, it is required to etch the specimen. Etching is the process of treating the surface of a sample with a chemical mixture (etchant) that reacts with the surface of the sample. Since not every material phase is equally reactive with the etchant, a difference in colours will develop between the different phases. Since atoms in the grain boundaries tend to be more chemical active than those within grains, small grooves will form in the locations of grain boundaries [21]. There is a wide variety of etchants available for etching aluminium alloys. Which etchant is most suitable, depends on the composition of an alloy.

Many common etchants for aluminium alloys, such as Keller's reagent, contain hydrofluoric acid. Due to safety concerns, the use of hydrofluoric acid (HF) is restricted in the lab where the specimens will be prepared. For this reason, a suitable HF-free etchant must be found. The composition of Scalmalloy is similar to that of 5000-series aluminium, with the exception that Scalmalloy contains a small percentage ($0.6\% - 0.8\%$) of scandium [15], to enhance mechanical properties. A specific difficulty for etching Scalmalloy is the very small grain size (in the range of $1\mu m$) that is typically present in some regions of additively manufactured Scalmalloy. It is very hard to etch material with such fine grain size and obtain desirable results. Some experiments were done to etch the material chemically, but a suitable HF-free etchant for Scalmalloy could not be found.

The most successful etching attempt on Scalmalloy made the the melt pool structure visible, but no grains could be seen due to the very fine grain structure of some regions (grain size $\sim 1\mu m$). For this reason, another method must be used to analyse the grain structure of Scalmalloy.

EBSD

Scanning Electron Microscopy (SEM) uses an electron beam to analyse the surface of a specimen. The surface structure of the material is obtained from how an electron beam

interacts with the specimen [21]. The magnification is suitable for observing features down to nanometer-scale. Electron backscatter diffraction (EBSD) is a variation of SEM that can be used to find the grain structure and orientation in a sample, since each grain diffracts the electron beam in a different angle. EBSD is more complicated than optical microscopy for obtaining grain structures, but it can be useful if a material is very hard to etch or if the grain structure is too fine for successful etching. Spierings et al. have shown that EBSD is capable of capturing the grain structure, as is shown in figure 4.2. Therefore, EBSD was chosen as the method to visualize the crystal structure of the Scalmalloy samples, since it had proved to be impossible to obtain a desirable result with etching.

For EBSD, it is necessary to cut the specimens and embed them in a resin that conducts electricity. An extremely smooth surface is required for good results, which made the polishing procedure more complicated than for the other analysis methods that require polishing.

4.5.6 Mechanical analysis

Micro-indentation is chosen as a method to map the local hardness of the samples. Fatigue cracking may be preceded by strain hardening, which can be detected by micro-indentation. It is also possible that micro-cracking within the material that is not visible by other methods can cause a local decrease of material properties. Micro-indentation is a miniaturized type of a conventional indentation hardness test that can be used to detect very local differences in hardness, for instance between two regions with different grain structures within one sample [23]. The micro indentation machine that is available in the mechanical testing lab at the University of Twente is not capable of measuring the indentation depth in situ, which makes it unsuitable for measuring stiffness of a material. Micro-indentation is defined as a indentation test with an indentation force smaller than $2N$ and an indentation depth greater than $200nm$.

If the indentation depth is smaller than $200nm$, the test is classified as nano-indentation [24]. For nano-indentation equipment, it is also more common to measure the indentation depth during the test, so it can be used to measure stiffness of a material [25].

4.6 Required preparation steps

Not al proposed analysis steps require the same sample preparation. Figure 4.5 shows which preparation steps are required for the different analysis methods that are chosen.

The cutting step for the archimedes density analysis and CT-scanning is needed because the original test plates are too large to fit in the analysis equipment for these methods. The samples also need to be cut for the polishing procedure, because they need to be embedded in discs with a maximum cross-section of $50mm$. The cutting is done with a scissor-type metal plate cutter. This can cause some plastic deformation around the cutting surface, but this will only be very locally near the cuts. Cutting does not cause any build-up of heat in the samples, so no change in crystal structure is expected outside the cutting region.

In order to polish the specimens, they must be embedded after they are cut. Struers EpoFix clear epoxy resin is be used for embedding in cups with a diameter of either $25mm$ or $50mm$. Polishing is done in multiple steps, starting with relatively coarse sandpaper (500 grit), and gradually moving towards finer sandpaper (4000 grit). Thereafter, diamond suspensions of 3 μm and $1\mu m$ are used successively. The final step is to polish with a $0.25\mu m$ OP-S solution in order to obtain a mirror-like finish. All polishing steps are performed on a Struers Tegramin-30 machine.

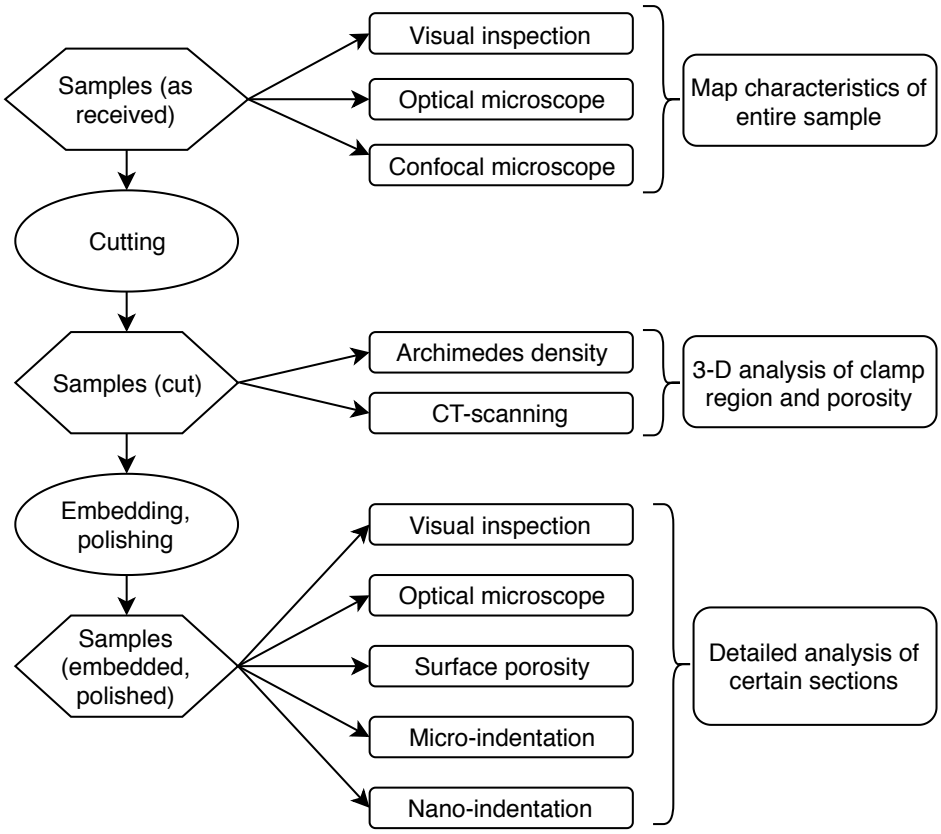

Figure 4.5: Sample preparation and analysis sequence.

5 | Analysis results

After the desired analysis methods were established, analysis of the samples was conducted as proposed in the previous chapter. This chapter will provide the results of each analysis method.

5.1 Initial analysis of as-received samples

The first analysis was performed without any specific sample preparation, except for some cleaning with isopropyl alcohol. This initial analysis step was very useful for getting an indication of the overall condition of the samples and to point out which regions are interesting for further analysis.

5.1.1 Visual inspection

All specimens were given a visual inspection to look for cracks and other types of damage. Each sample showed some surface scratches in the clamping region. In some samples, cracking was visible with the naked eye, but this was not immediately obvious for all specimens. Analysis under a microscope was required to get insight in the actual extent of these cracks and to determine their size.

5.1.2 Optical microscope

The optical microscope analysis was performed on a Keyence VXH-5000 microscope. A lens was fitted that allowed for a magnification factor between 100× and 1000×. All specimens were examined from the rear side, since markings were applied on the front, making it hard to identify damage on that side.

Each sample was reviewed under the optical microscope without any specific specimen preparation. First, the clamping regions in each specimen were scanned with a magnification of 200×. The regions of interest were identified and observed under greater magnification if more detail was desired. Snapshots were taken of the most interesting regions of each specimen, with various different magnifications per snapshot. After this inspection, the following remarks could be made:

- All 13 Scalmalloy specimens that endured 300.000 load cycles or more showed significant fatigue cracking.
- One out of three Scalmalloy specimen showed a beginning fatigue crack after only 75.000 cycles, two out of three showed cracking after 150.000 cycles.
- 7 out of 8 Al 7075-samples show fatigue cracking, the only exception is the b-side of specimen 1005, which had undergone $300,000$ cycles.

The Scalmalloy specimens were printed in a larger thickness than the desired test specimen size, so they were machined down to the final thickness of $1mm$. The machining process left a circular pattern on the surface of the specimens that is clearly visible. In the regions where the angle between the circular machining marks and the clamping direction is smaller

than approximately 20°, the cracks tend to follow the machining marks. An area where this behaviour could be observes is shown in figure 5.1.

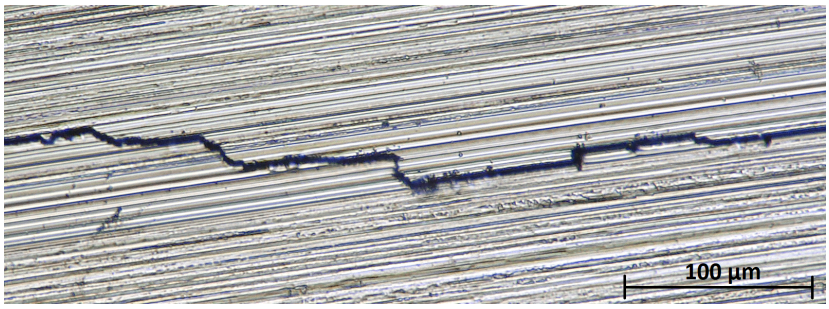

Figure 5.1: Crack following machining marks on the surface of sample 6901-6a.

5.1.3 Confocal microscope

The confocal microscope was able to capture a more detailed image of the cracks that were already observed with the optical microscope, but no indications could be found that cracks are actually longer than they appeared under the optical microscope. A major advantage of confocal microscopy is the capability to capture the surface profile in three dimensions up to a high resolution, which is particularly useful for roughness analysis. An example of a confocal microscopy image of sample 6901-9a is shown in figure 5.2. A fatigue crack is visible near the right side of the image, and the machining marks are clearly visible over the entire surface.

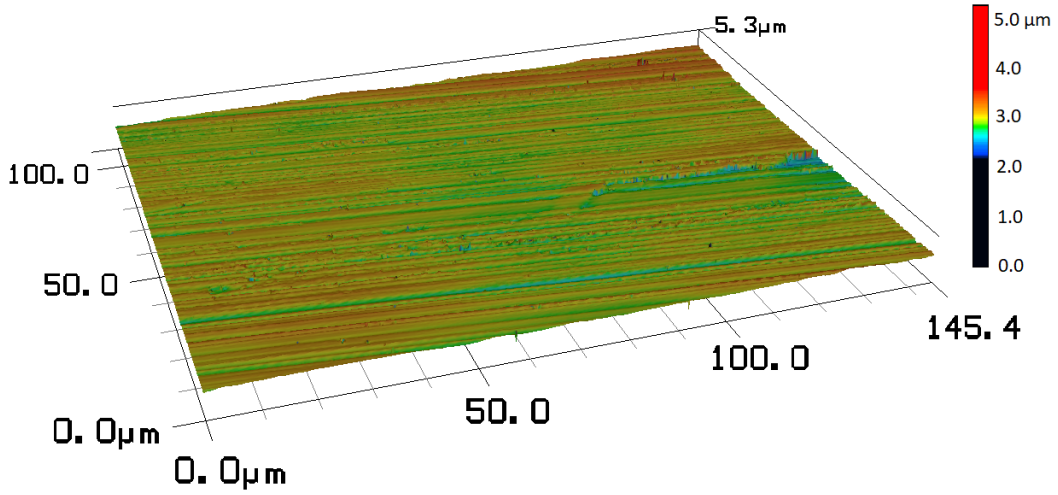

Figure 5.2: Example of a height profile obtained by confocal microscopy (sample 6901-9a).

Roughness development in fatigue affected area

To find whether surface roughness can be used as a damage precursor, the influence of fatigue on several surface roughness parameters was determined. To this end, ten confocal microscope images were taken of regions in the samples that were not affected by fatigue and eight images from regions that were fatigue affected, but did not show any sign of damage. Several different roughness parameters were registered using the confocal microscope image processing

software, including roughness average (Ra), root mean square of roughness (Rq), maximum profile height (Rz), and kurtosis of roughness (Rku). The mathematical definitions of these parameters, based on local height measurements y_i are given in equations 5.1 till 5.4.

$$Ra = \frac{1}{n}\sum_{i=1}^{n}|y_i| \tag{5.1}$$

$$Rq = \sqrt{\frac{1}{n}\sum_{i=1}^{n}y_i^2} \tag{5.2}$$

$$Rz = Rp + Rv \tag{5.3}$$

With Rp the maximum peak height and Rv the maximum valley depth.

$$Rku = \frac{1}{nRq^4}\sum_{i=1}^{n}y_i^4 \tag{5.4}$$

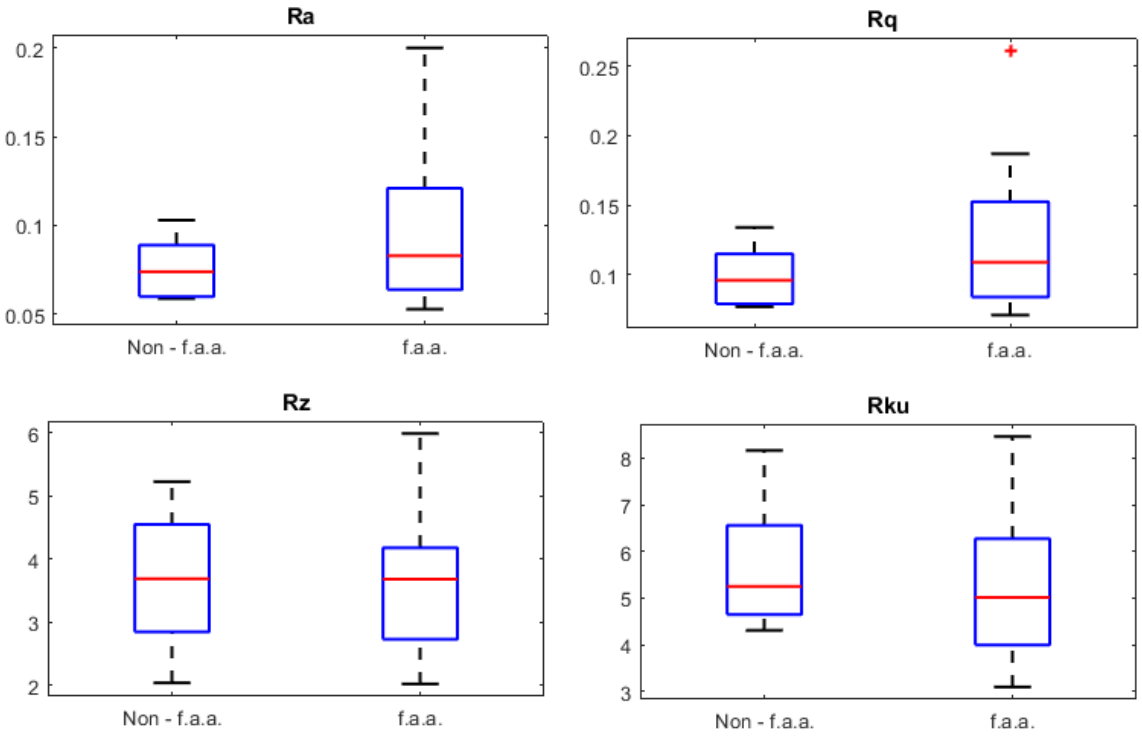

Figure 5.3: Roughness parameters for Scalmalloy

Figure 5.3 shows box plots of the roughness measurements. The roughness measurements in fatigue affected areas show a larger spread of most roughness parameters, but there are also several examples where the roughness in the fatigue affected areas is equal to, or even lower than the roughness outside these areas. For this reason, it is not possible to make a reliable distinction between fatigue affected and non-fatigue affected areas solely based on surface roughness parameters.

5.2 Analysis of fatigued samples after cutting

After the first inspections, some samples were cut into pieces for density analysis using the Archimedes method and detailed analysis of the inside of the material by CT-scanning.

5.2.1 Archimedes density analysis

The density of several samples was calculated with the Archimedes density method that is described in chapter 4. From each batch, three similarly sized samples were used with an average sample mass of $0.71g$ before application of lacquer. The density of the lacquer was calculated by comparing the weight and density of an aluminium sample with and without lacquer. To this end, regular extruded aluminium samples were used, so that the accuracy of measurements cannot be influenced by porosity in the aluminium. The density of the lacquer was calculated to be $1.287g/cm^3$. The results of the Archimedes density analysis for the different batches of Scalmalloy are in table 5.1.

Sample	Powder condition	Density (avg.)	Standard deviation	Porosity (avg.)
6901	Re-used, not dried	$2.6655g/cm^3$	$3.7466 * 10^{-3}g/cm^3$	0.167%
6902	Virgin	$2.6635g/cm^3$	$5.6105 * 10^{-3}g/cm^3$	0.247%
6903	Re-used, dried	$2.6607g/cm^3$	$4.2961 * 10^{-3}g/cm^3$	0.347%

Table 5.1: Porosity calculated using the Archimedes method.

These results suggest that the powder of lowest theoretical quality (re-used-not dried) results in products with the highest density when compared to virgin or re-used and dried powder. This is in contradiction to results that were presented on papers on the subject of powder drying [17] [19]. However, the standard deviation of the measurements from each batch suggests that the measured difference might also be attributed to measurement inaccuracies. At least, it can be concluded that there is no huge difference between densities of the three different batches of Scalmalloy.

5.2.2 CT-scan

From sample 6902-3a, the fatigued area was cut out and scanned in a CT-scanner at the Sandia National Laboratories in Albuquerque. Measurements were performed in-plane and out of plane. The in-plane measurements yielded the most comprehensive results, and clearly showed the fatigue cracks and porosity in this Scalmalloy sample. The individual frames from the in-plane measurement could be stacked on top of each other to re-construct a three-dimensional model of the sample. This was done using Matlab, and the results are shown in figure 5.4. In the right half, a crack is visible that spans the entire thickness of the sample. On the left, there is another crack visible that spans approximately half the specimen depth. Most of the black spots represent pores in the material.

When the regions that contain cracking are excluded from the image, the porosity percentage over the entire volume of the sample can be estimated by counting the percentage of pixels in the cross-section that is black. For the one sample that was CT-scanned, a porosity of 0.034% was calculated with this method. The resolution of the CT-scan was 2464 by 1380 pixels for an area of approximately $1500mm^2$, so each pixel represents an area of $\sim 21\mu m$ by $21\mu m$. The majority of pores that are smaller than this size are not visible on the CT-images, which could explain the large difference compared to the other porosity analysis

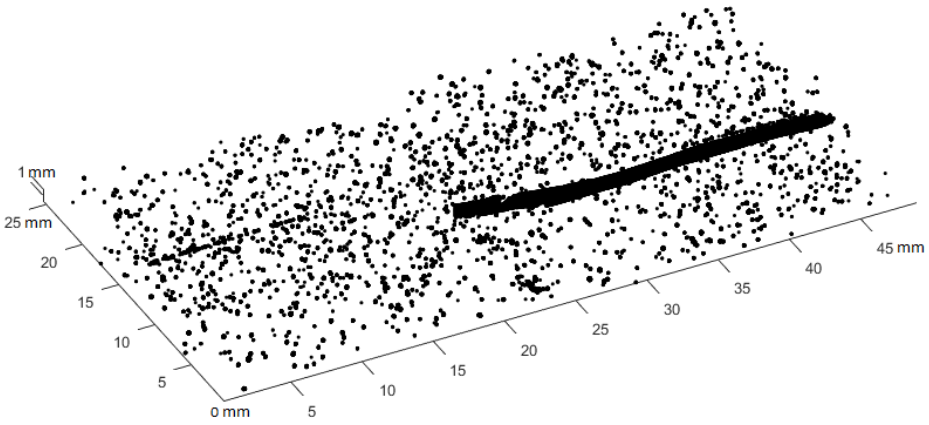

Figure 5.4: 3D-map of CT-scan of sample 6902-3a. Axis dimensions are in millimetres.

methods. Another potential cause of inaccuracy is the threshold that was used for converting the original grey scale image to a black-and-white image.

The presence of cracks and porosity was already clearly before CT-scanning, and no other behaviour was observed that could indicate the presence of damage precursors. However, it was very useful to see the depth of the cracks, which could be especially useful for samples with greater thickness than the test plates that were used in this experiment.

5.3 Analysis of polished samples

For further examination, certain portions of the test plates were embedded and polished. A conductive resin was used for some samples in order to analyse the grain structure using EBSD analysis in a scanning electron microscope.

5.3.1 Visual inspection

The smooth surface that was obtained by polishing made it possible to observe some irregularities in the surface with the naked eye. Most easily visible were the deep cracks in the fully fatigued samples, but these were already visible before polishing. Upon closer examination in suitable lighting conditions, it was also possible to see some porosity with the naked eye.

A drawback of the polishing procedure for partly fatigued samples is that it removes material from the surface. Since not all cracks run through the entire thickness of the specimens, some small cracks had disappeared after the polishing process.

5.3.2 Optical microscope

The difference between the polished and as-received samples becomes clear when the specimens are observed under the optical microscope. In figure 5.5, a section of sample 6902-4a is shown before and after polishing.

The comparison in figure 5.5 shows that polishing provides more detail in cracked areas, especially where clamping marks from the fatigue testing were present before polishing. The unpolished samples showed no sign of porosity, but a significant amount of porosity was revealed after polishing.

(a) Before polishing.

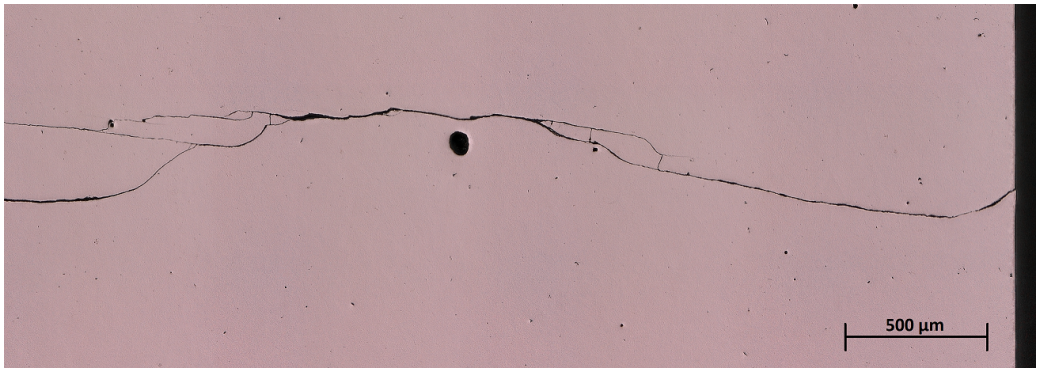

(b) After polishing, the large pore in the middle has a cross-section of $\sim 80\mu m$.

Figure 5.5: Comparison between microscope image of cracked area before and after polishing in sample 6902-4a.

Crack development in clamp area

Before polishing, it was hard to see how the cracks developed in the clamp area due to the large amount of surface scratches in the clamping region. This scratching was removed by the polishing process, greatly improving visibility of scratches in these areas. The cracks in the clamp region tend to be more split than cracks that appeared outside the clamping region. This indicates that the clamp has had a significant influence on how fatigue cracks developed.

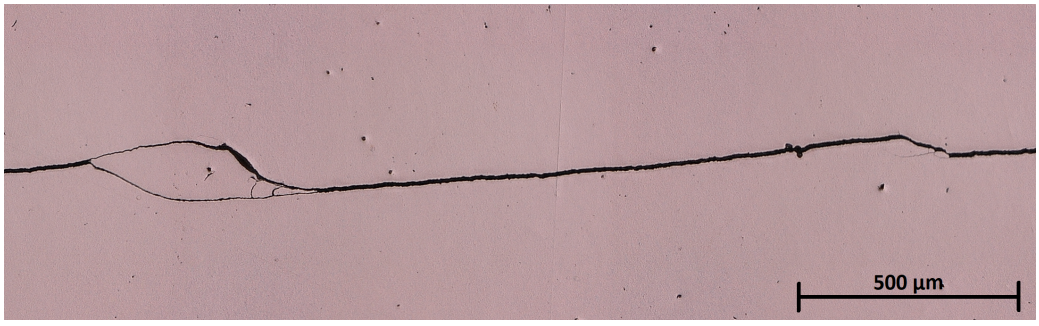

Figure 5.6: Split cracks in clamp region that showed up after polishing (sample 6903-3A)

A common type of cracking behaviour that is observed in the clamp region is overlapping and merging crack patterns that tend to form 'islands' of material surrounded by two cracks. An example of this behaviour is shown in figure 5.6. This behaviour does not occur outside

the clamp regions, where the cracks tend run continuously with very little branching. The odd cracking behaviour in the clamp regions is probably caused by the clamping beams that are made from steel, which is a much harder material than the aluminium test specimens. If the steel clamp slightly digs into the aluminium specimen, it causes a local stress concentration, accelerating the growth of fatigue cracks in that region. This effect is intensified by the fact that the screws that close the clamp are spaced quite far apart, which causes more pressure around the edges of the test specimens, where the most severe cracking was observed.

Attempt to avoid local influence of clamp

To see if it was possible to move the crack area outside the clamp region without making major alterations to the test method, a hole with a cross-section of $0.6mm$ was drilled close to the clamp region of a test plate before fatigue testing. The stress concentration that is caused by an elliptical hole can be calculated using equation 5.5, with σ_m the maximum stress at the tip of the hole, σ_0 the nominal stress, a half the width of the hole and ρ_t the radius at the tip of the hole.

$$\sigma_m = 2\sigma_0\sqrt{\frac{a}{\rho_t}} \tag{5.5}$$

Since a circle is an ellipse with ratio $\frac{a}{\rho_t}$ equal to 1, a circular hole will cause a local stress concentration that is twice the nominal stress in the plate. However, the test plate with the hole showed the same cracking behaviour in the clamp region. From this, it can be concluded that the local stress concentration caused by the clamp has more influence than the stress concentration caused by the hole near the clamp region, and a different method must be found to remove the influence that the clamp has on crack growth.

Influence of porosity on crack growth

The polishing process made a significant amount of surface porosity visible, which made it possible to estimate the influence of pores on crack growth. Most pores are rather small, roughly between $5\mu m$ and $30\mu m$ and there was almost no visible interconnectivity between pores. However, there are also a few larger pores up to a cross-section of $100\mu m$ present in all specimens. Since the specimens were initially $1mm$ thick, a maximum of 10% of the sample thickness is occupied by a single pore.

There is no visible evidence that the cracking is influenced significantly by the presence of pores. Cracks do not seem to be attracted significantly to pores, and there are no big changes in crack direction if a crack runs through a pore.

5.3.3 Surface porosity analysis

In order to determine the properties of non-fatigued material, a number of samples from the central area of several specimens were embedded and polished. After this process, the porosity of the material could be evaluated under a microscope. An example of such a micrograph is in figure 5.7. The black spots in this image are pores that show up in the polished surface. To make it easier to estimate the percentage of surface porosity, some image manipulation was performed to transform the original coloured micrograph into a black-and-white image. By counting the percentage of black pixels in the image, an estimation of the porosity percentage could be obtained. This method is not perfect, since it makes no distinction between pores and dark spots in the image, that could be caused by other features, such as precipitates.

Since the procedure was identical for all specimens, it is reckoned to be a suitable method for comparison of different specimens.

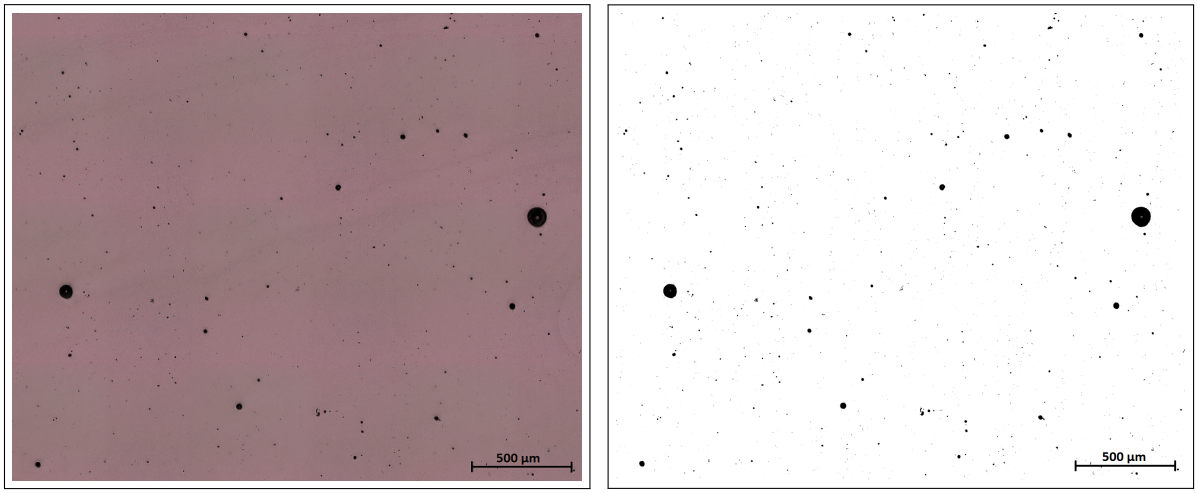

Figure 5.7: Part of micrograph from polished Scalmalloy on the left. Converted image for better porosity detection on the right.

The results of the surface porosity analysis are in table 5.2.

Sample	Powder condition	Measured area	Porosity percentage
6901-8	Re-used, not dried	$100.8mm^2$	0.533%
6902-3	Virgin	$92.2mm^2$	0.207%
6903-1	Re-used, dried	$86.7mm^2$	0.282%

Table 5.2: Surface porosity of measured samples

This analysis indicates that the porosity of the material from virgin powder is the lowest, and that drying has a positive influence on porosity of the printed material. The porosity percentages of the 6902 and 6903 samples are in the same order of magnitude compared to the Archimedes method, but there is a significant difference for the 6901 samples. Since the Archimedes density method is very susceptible to small measurement errors, it is reckoned that the optical porosity results are more reliable than those obtained by the Archimedes method.

5.3.4 Micro-indentation

To find whether the hardness of the material is influenced by fatigue, micro indentation hardness tests were performed. To find local differences and to compensate for local variations, multiple indentations were made in a grid pattern, as is shown in figure 5.8.

Hardness tests were performed for samples from all three different Scalmalloy batches (re-used, virgin and dried), and for a conventionally manufactured Al 7075 sample. In each sample, 48 indentations were made, in groups of 8. Each group was placed on the same distance from a fatigue crack ($0.1mm$, $0.25mm$, $0.5mm$, $0.75mm$, and $1mm$). Additionally, there were groups of 8 indentations placed inside the crack and at a distance far away ($\sim 10mm$) from the crack, making the total number of indentations 56. The indentations were placed in groups of 8 to rule out local variations in properties. The indentations in the crack and far away from the fatigue affected area are not shown in figure 5.8, since they were done

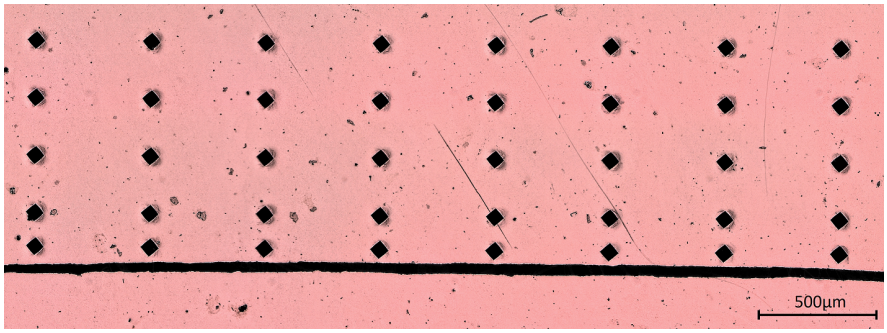

Figure 5.8: Example of the used indentation grid.

separately. The indentation grid was placed parallel to an existing fatigue crack, so that each row of 8 indentations was placed in the same distance from the crack.

The results of the micro hardness tests are displayed in figure 5.9. It these box plots, the red line in the centre of each box represents the median of the corresponding set of measurements, the upper and lower edges of the boxes represent the 25 and 75 percentiles and the ends of the whiskers correspond to data points that are not considered to be outliers. The red + markings correspond to outliers in the data set.

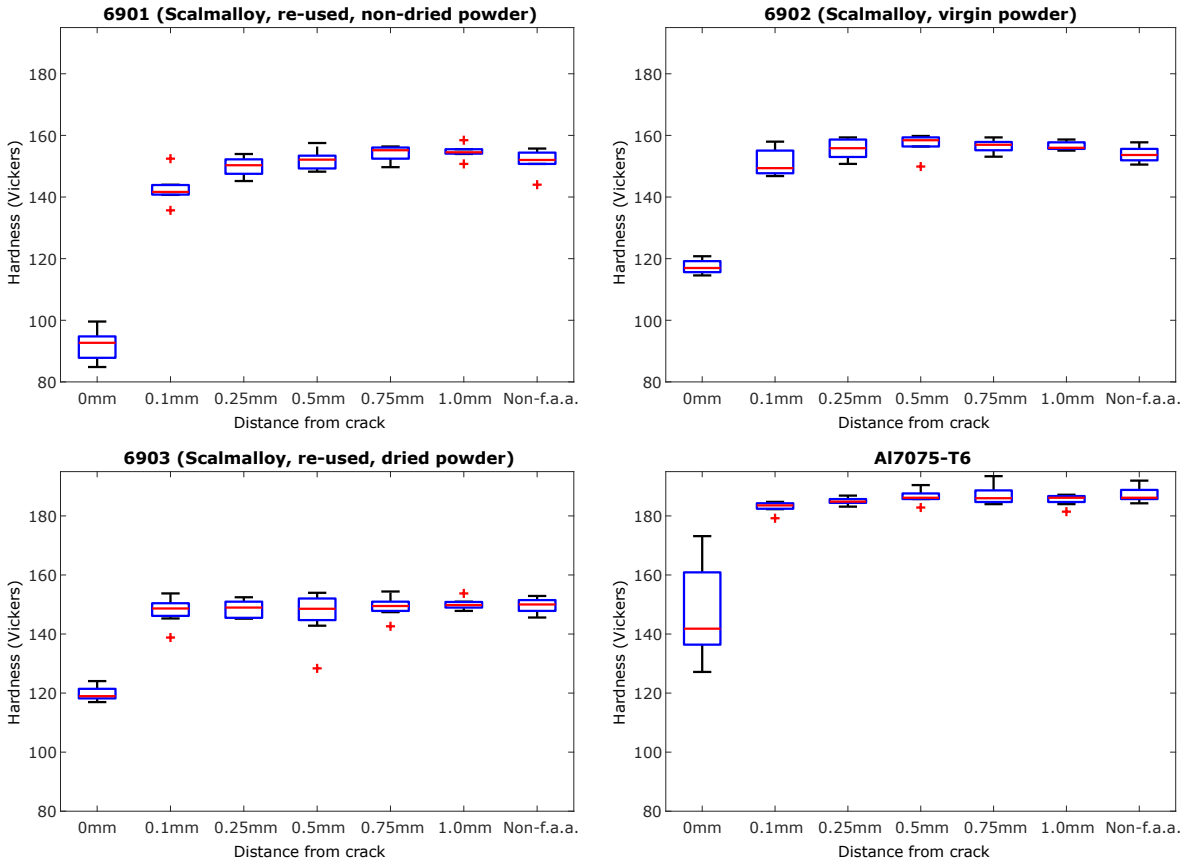

Figure 5.9: Results of micro hardness tests.

To evaluate the influence that surface porosity can have on the hardness measurements, one micro-indent was placed deliberately inside a large pore. In this pore, a hardness of $51.36HV$ was measured. In a smaller pore, a hardness of $132.69HV$ was measured. This

shows that porosity can have a significant influence on the result of a micro indentation measurement if a pore is present in the area of indentation, because a lower value will be measured due to absence of solid material in the pore. This can explain the larger spread in hardness measurements observed in Scalmalloy compared to conventional Al 7075-T6, since almost no porosity is present in the conventionally produced aluminium, thus making the measurements more consistent.

The measured hardness in the cracked regions is significantly lower than in all other regions, but this is probably due to the indentation tip sinking in the crack in stead of a decreased hardness of the material itself. The rest of the measurements does not show an unambiguous relation between the measured hardness and distance from fatigue crack. In the 6901, 6902 and 7075 samples, there is a slightly increasing trend visible between $0.1mm$ and $0.5mm$, but this is not present in the 6903 set and the increase in the 7075 set is extremely small.

5.4 Nano-indentation

Since the micro-indentation equipment was not capable of measuring indentation depth in relation to indentation force during the measurement, the only material parameter that could be measured with this equipment is the local material hardness. If the indentation force can be plotted against indentation depth in a load-displacement curve, it can be checked whether the Young's modulus is affected by fatigue, even if the hardness remains unchanged. In a conference paper of Haynes et.al [26], a decrease of stiffness was found close to an existing fatigue crack. To test whether such a relation is present in the samples that were used for this work, two tests were analysed using nano-indentation equipment. The results of these tests are shown in figure 5.10.

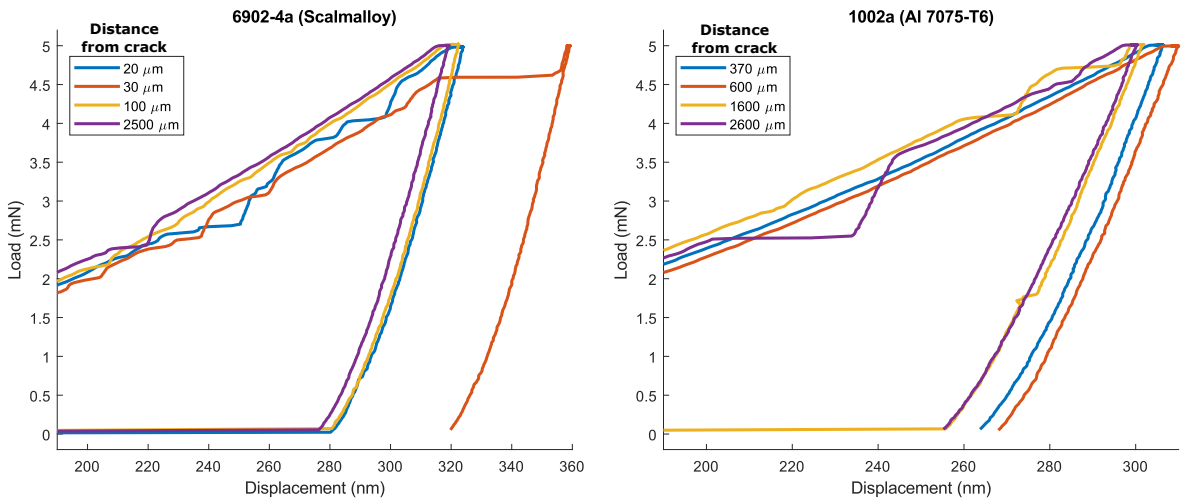

Figure 5.10: Results of nano-indentation on Scalmalloy and Al 7075-T6.

These graphs can be divided into two parts: a gradual inclination from the left side towards the top right corner as the load is gradually increased, and a steep drop when the load is decreased. The slope of the graphs upon release of the load is directly correlated to the Young's modulus of the material, as it springs back slightly upon release of the indentation tip. The point in the graph where the indentation force has gone back to zero indicates the amount of plastic deformation that the indenter has caused.

If the stiffness of material would have degraded as a result of fatigue, the downward inclination of the graphs would have been steeper for indentations further away from a fatigue crack. This relation was not present after the first nano-indentation experiments on Scalmalloy and Al 7075-T6, so it was concluded that nano-indentation would not give any different results than the micro-indentation analysis had already provided.

5.5 EBSD analysis of grain structure

To see how the grain structure interacts with the fatigue behaviour of Scalmalloy, an EBSD analysis was performed on a sample that contained a beginning fatigue crack. The sample in case was 6901-9b, which contained a single fatigue crack over a length of approximately $10mm$. An EBSD image was made over an area of approximately $47.0\mu m$ by $22\mu m$, as is shown in figure 5.11.

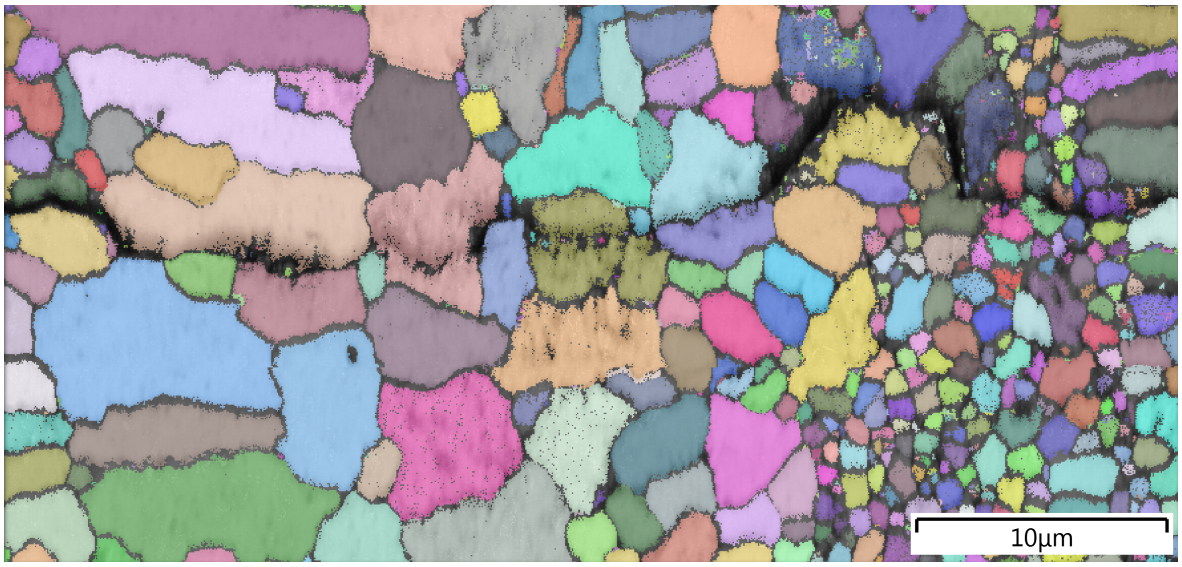

Figure 5.11: EBSD image of fatigue crack in Scalmalloy

The EBSD image shows that the same division in fine-grained and coarse-grained areas that was found in literature [14] is present in the test specimens. The crack is clearly visible central in the image and it can be seen that the crack follows the grain boundaries (intergranular fracture) in the areas with fine grains. In the coarse grained regions, a combination of intergranular and transgranular fracture is can be seen. In order to see if the grain structure changes before cracking occurs, an attempt was made to take an additional EBSD-image of the tip of a fatigue crack. However, the crack becomes very narrow near the tip, the EBSD equipment struggled to capture the grain boundaries with sufficient sharpness. Therefore, it became impossible do distinguish the crack tip from regular grain boundaries. Therefore, it was concluded that it is not practical to use changes in grain structure for the purpose of damage precursor detection.

5.6 summary of measurement results

In this chapter, the results of all measurements that were proposed in chapter 4 were presented. The goal of the measurements was to characterize the different batches of material

and to find out which changes develop in the material before fatigue cracking starts to occur. This section gives a brief summary of the most relevant results that were obtained.

The optical microscope turned out to be a very capable method to analyse the presence of cracks in the test samples. Polishing did help improve visibility of the cracks, but it only revealed features that were previously not visible in the clamp area. The confocal microscope did not reveal cracks and other features that were not visible with the optical microscope, but the high depth resolution did make it possible to analyse roughness parameters. No evidence was found that roughness parameters can be reliably used as damage precursors.

Three different methods were used to analyse porosity in the samples. The optical surface porosity measurement and the Archimedes density method provided results of similar orders of magnitude. The results obtained with the optical method were in line with what was expected based on the condition of powder that was used to produce each set of samples, and the results from this method are less prone to measurement errors and easier to verify after the test has been taken. The third method that is (in theory) capable of visualizing porosity is CT-scanning, but the resolution that was used, was too low to provide usable results. The CT-scan was mainly useful for finding cracks that are not on the specimen surface, but it did not reveal anything that could not be seen using optical microscopy.

Indentation tests were carried out to see whether fatigue has had a measurable influence on local hardness. No major relation could be found between hardness and distance from an existing fatigue crack, and also no influence of fatigue on the Young's modulus could was found in the load-displacement curves that ware obtained using nano-indentation.

6 Discussion of measurement results

This chapter will discuss the results that are presented in chapter 5, and some attention will be given to the practical implications of these results.

6.1 Knowledge about damage precursors

One of the major objectives for this work was to gather insight in the development of damage precursors. After a general investigation about the possible approaches to define damage precursors, it was chosen to focus on searching for physical changes in the material before the development of visible fatigue cracks. Various methods were applied to find how the material has changed after the fatigue tests.

6.1.1 Optical microscopy

Using a relatively straight-forward optical microscope, it was found early on that more cracks were present in most of the samples than was expected based on the dynamic results that were obtained during previous experiments. This knowledge triggered a renewed interest in the dynamic results that were obtained when the test samples were subjected to fatigue loads. It turned out that the early fatigue cracks could be traced back in the dynamic results, in the form of minor frequency shifts that occurred in some higher vibration modes. This confirms that it is very useful to use an integrated approach where dynamic results are verified by optical methods.

6.1.2 Micro- and nano-indentation

Indentation experiments were done to find how the hardness of the material had changed after the fatigue tests. The main reason to do this, was the graph in figure 6.1 that was presented by Haynes et al. [26] and a mention of similar behaviour by Habtour et al. [27].

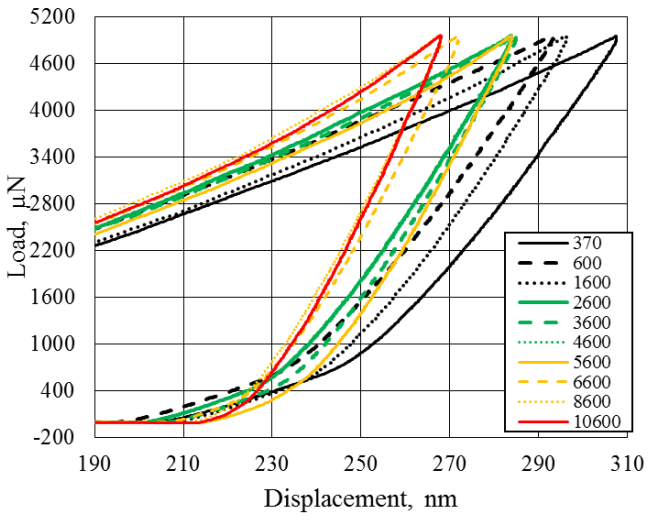

Figure 6.1: Nano-indentation results obtained by Haynes et al. [26] Units are in μm.

In figure 6.1, results of nano-indentations are shown where indentations were placed in a Al 7075-T6 sample. Each line in the graph represents a different distance from a fatigue affected area. a clear difference in downward slopes is visible as indentations are placed further away from a fatigue affected area. This suggests that the Young's modulus is lower at positions close to the fatigue affected area. It was tried to repeat this experiments on both Scalmalloy and Al 7075-T6 samples that were studied in this work, but no similar relation could be found. The reason for the different results is not clear, but it might be due to differences in equipment or the method that was used to subject the samples to fatigue loads.

6.2 Influence of AM parameters on fatigue behaviour

The additively manufactured samples were made from three different batches of powder with varying powder conditions. In theory, the powder that has never been used before (virgin) results in higher quality of the printed product when compared to re-used powder. The most relevant parameter where this difference in quality can be measured is the porosity of material after printing. Three methods were employed to measure the porosity. Of these three methods, the optical method was the only one that clearly showed the expected distribution of porosity. However, the Archimedes density method indicated that the density of material printed with the lowest quality powder was the highest, but the standard deviation of these measurements could explain this as a measurement error. One sample was analysed using a CT-scan, but the resolution of these images was too low to draw any reliable conclusions about the density of the sample.

In theory, high porosity could cause acceleration of fatigue damage as the pores could act as a point of stress concentration, but no clear evidence was found that porosity had a major influence on the development of fatigue cracks. The experiment with a sample that had a hole drilled in it, could be considered as an extreme example of the presence of one very large pore. However, even with a hole very close to the clamp, it did not act as a fatigue initiator despite doubling the local stress in the material. This could be explained by the local stress that is caused by the clamp. The only ways to eliminate this effect, would be to re-design either the clamp or the test plate. If the influence of the clamp is eliminated, it might be feasible to print specimens with a larger spread in porosity than the current test plates. By subjecting these plates to equal amounts of fatigue load, the actual influence of porosity of fatigue crack growth could become apparent.

6.3 Usability of results for maintenance optimization

The ultimate goal of a gathering understanding of damage precursors is the increase of reliability an optimization of maintenance policies. The implications of the obtained results are discussed here, along with some guidelines that must be taken into account when damage precursors will be applied in practise.

6.3.1 Application of results in practise

The analysis methods that were applied did not all yield useful knowledge about the development of damage precursors. The most useful result was the discovery that cracks were already present in earlier stages than expected based on the dynamic results. However, this does not mean that optical analysis is the most suitable method for detecting damage precursors because it requires direct access to the component that is analysed. For practical applications, this means that removal of a component from a machine is required in order to

perform these analysis methods. This will likely cause excessive downtime and thus increase overall operation costs, making the application of damage precursors less feasible. This drawback can possibly be avoided when the dynamic approach is used, because it is possible to measure dynamic response of a component when it is in operation, if a suitable monitoring method is used. The main purpose of optical microscopy will therefore be for the verification of the dynamic approach, but not for regular inspections.

The other methods that were applied did not contribute to finding damage before cracking appeared, and share the drawback with optical microscopy that components need to be removed in order to apply analysis methods. Furthermore, some of these methods are destructive to some extent.

6.3.2 Guidelines for successful application of damage precursors

To apply damage precursors successfully, there are several important factors to take into account for obtaining a satisfactory result. There are several questions that are useful to ask before the decision is made to apply damage precursors.

Which components are suitable for application of damage precursors?

Not every component is equally suitable for application of damage precursors. It is not useful to choose components that never fail in practise, or when the degradation behaviour is very well known, for instance in the case of easily visible wear. It is also important that the component is made from a material where the degradation behaviour is well known, because otherwise there is no way of knowing what behaviour is expected before damage occurs.

How is the component expected to fail?

Once a component is selected for application of damage precursors, it must be known how it is expected to fail. Components that always tend to fail in the same manner are the most suitable for application of damage precursors. It should be known how damage precursors manifest in the component and how they could be detected. For components that have several different failure modes in practise, each possible failure mode must be monitored individually for damage precursors.

What type of damage precursor is the most feasible?

As discussed, there are different approaches possible to define damage precursors. Not every approach is equally feasible for all applications, so it is important to select the most suitable approach for the component that is selected for application of damage precursors. Even though the experiments that are described in this report were focusing on detecting changes in physical properties before fatigue cracking occurs, it is likely that the dynamic approach is most feasible for practical applications.

What is the expected improvement when damage precursors are used?

Before it is decided to apply damage precursors on a component, it is necessary to investigate in advance what improvement could be made regarding either maintenance costs or reliability of the system. Damage precursors have the possibility to improve both aspects, but if expensive inspection methods or sensor arrays are needed for investigating whether damage precursors are present, it might be cheaper to use a difference maintenance policy in stead.

7 Conclusions and recommendations

7.1 Conclusions

Several conclusions can be drawn from the research that was presented in this work. The conclusions will be given in the same order as the research objectives were formulated.

7.1.1 Approaches to define damage precursors

The first research objective was about the definition of damage precursors. Three approaches were presented on how the subject damage precursors can be approached:

- Base damage precursors on changes in dynamic response
- Base damage precursors on changes in physical properties of the material
- Use a definition for damage precursors based on the reliability of a component

Although the approaches are different, there is a link present between all three approaches. This report has mainly focussed in finding the link between a change in dynamic and physical properties, in order to find how the material has changed once a certain dynamic behaviour is observed. It is likely that the dynamic approach is the most feasible method to use in practical applications.

7.1.2 Observed changes in physical properties

The following methods were applied in order to find physical changes in the sampoles after fatigue testing:

- Visual inspection
- Optical microscopy
- Confocal microscopy
- Archimedes density analysis
- CT-scanning
- Surface porosity analysis
- Micro-indentation
- Nano-indentation

It turned out that significant fatigue cracking could be observed with the optical microscope when only subtle changes in higher-order dynamic properties were noticeable. Confocal microscopy did not yield any relevant information that could not be obtained with optical microscopy. The optical surface porosity analysis method tuned out to be the most accurate method of analysing porosity, as the Archimedes method was quite susceptible to small measurement errors and the resolution of the CT-scans was insufficient. The porosity percentage

of the samples was quite low, and the small amount of porosity that was present did not seem to have a major influence on fatigue crack growth. No major change in hardness and Young's modulus was found close to existing fatigue cracks after the indentation tests, which was an unexpected result when compared to results that were available in literature [26].

7.1.3 Implementation to optimize maintenance parameters

It depends on a variety of factors whether it is feasible to apply damage precursors in regular applications. Based on the results of the experiments, it is unlikely to be feasible that changes in material properties can be used as damage precursors. The need to remove components in order to inspect them is also a major drawback of most of the used analysis methods. Actual implementation of damage precursors would therefore rely on a more thorough understanding of the link between dynamic changes and changes in physical properties than what is currently available.

7.2 Recommendations

Based on the observations during this assignment, several recommendations can be formulated to improve further research and to aid successful implementation of damage precursors in practical applications.

7.2.1 Improvement of future fatigue experiments

The test plates that were used for this assignment had a uniform width and thickness and were fixed in a steel clamp during experiments. This caused stress concentration in the clamp region, causing the beams to crack right at the clamp region. This is undesirable, because it introduces several factors that can influence the results of the experiments. During the course of the assignment, an experiment was done with a small hole drilled a small distance away from the clamp region in order to initiate fatigue fracture at this hole. However, this did not yield the desired result.

A better approach would be to use different test plates for future experiments that are either wider or thicker at the clamp region, to decrease the stress in that region. If the test plates are better designed, they will start to crack outside the clamp region, thus eliminating cracks caused by local stress concentrations in the clamp region. This eliminates local differences caused by the clamp, and makes it easier to compare different results.

7.2.2 Try application of damage precursors in a real use-case

The experiments that are presented in this report are all done on test plates that have been subjected to artificial fatigue cycles. This is very good for getting a better understanding in the behaviour of material, but there is no real applications where similar plates are subjected to these loads. Therefore, it can be useful to pick a practical situation where a component is subjected to a fatigue load and try to find damage precursors for predicting fatigue failures. Since practical use-cases will be less predictable than artificial fatigue tests, it is likely that some new challenges will arise that need to be addressed before damage precursors can be successfully be applied on a large scale.

References

[1] Ed Habtour, Daniel P. Cole, Samuel C. Stanton, Raman Sridharan, and Abhijit Dasgupta. Damage precursor detection for structures subjected to rotational base vibration. *International journal of non-linear mechanics*, 82:49–58, 2016.

[2] Thiago Dragman. Identifying dynamic nonlinearities due to damage precursors in flexible structures. Master's thesis, University of Twente, April 2019. An optional note.

[3] Lokilech. Pedalarm bruch, June 2007. License: Creative Commons BY-SA 3.0.

[4] Ian Gibson, David Rosen, and Brent Stucker. *Additive Manufacturing Technologies. 3D Printing, Rapid Prototyping, and Direct Digital Manufacturing.* 2nd edition, 2015.

[5] C.R. Farrar, H. Sohn, and G. Park. *Converting Large Sensor Array Data into Structural Health Information.* DEStch Publications, Inc., 2005.

[6] J. Moubray. *Reliability-Centered Maintanance.* Butterworth-Heinemann, 1999.

[7] Tiedo Tinga. *Principles of loads and failure mechanisms. Applications in maintenance, reliability and design.* Springer Series in Reliability Engineering. Springer, 2013.

[8] D.C. Montgomery and Runger G.C. *Applied Statistics and Probability for Engineers.* Wiley and Sons, 5th edition, 2011.

[9] David Eccles. Sls system schematic, October 2018. License: Creative Commons BY-SA 4.0.

[10] John O. Milewski. *Additive Manufacturing of Metals*, volume 258. 01 2017.

[11] Li Yang, Keng Hsu, Brian Baughman, Donald Godfrey, Francisco Medina, Mamballykalathil Menon, and Soeren Wiener. *Additive Manufacturing of Metals: The Technology, Materials, Design and Production.* 01 2017.

[12] APWORKS GmbH. Scalmalloy material data sheet, July 2019.

[13] Granta Design Limited. Ces edupack, 2019.

[14] Adriaan Spierings, Karl Dawson, Thorsten Heeling, Peter Uggowitzer, Robin Schäublin, Frank Palm, and Konrad Wegener. Microstructural features of sc- and zr-modified al-mg alloys processed by selective laser melting. *Materials and Design*, 115, 11 2016.

[15] Mustafa Awd, Jochen Tenkamp, Markus Hirtler, Shafaqat Siddique, Markus Bambach, and Frank Walther. Comparison of microstructure and mechanical properties of scalmalloy produced by selective laser melting and laser metal deposition. *Materials*, 11, 12 2017.

[16] Maria Montero-Sistiaga, Raya Mertens, Bey Vrancken, Xiebin Wang, Brecht Hooreweder, Jean-Pierre Kruth, and Jan Humbeeck. Changing the alloy composition of a17075 for better processability by selective laser melting. *Journal of Materials Processing Technology*, 238, 08 2016.

[17] Christian Weingarten, Damien Buchbinder, Norbert Pirch, Wilhelm Meiners, Konrad Wissenbach, and Reinhart Poprawe. Formation and reduction of hydrogen porosity during selective laser melting of alsi10mg. *Journal of Materials Processing Technology*, 221, 07 2015.

[18] Laura Cordova, Mónica Campos, and Tiedo Tinga. Assessment of moisture content and its influence on laser beam melting feedstock. 10 2017.

[19] Xiaopeng Li, K.M. O'Donnell, and Tim Sercombe. Selective laser melting of al-12si alloy: Enhanced densification via powder drying. *Additive Manufacturing*, 10, 02 2016.

[20] Wessel Wits, Simone Carmignato, Filippo Zanini, and T Vaneker. Porosity testing methods for the quality assessment of selective laser melted parts. *CIRP Annals - Manufacturing Technology*, pages 201–204, 06 2016.

[21] William D. Callister and David G. Rethwisch. *Materials Science and Engineering*. Wiley, 8th edition, 2011.

[22] Adriaan Spierings, M Schneider, and R Eggenberger. Comparison of density measurement techniques for additive manufactured metallic parts. *Rapid Prototyping Journal*, 17:380–386, 08 2011.

[23] James Best, Xavier Maeder, Johann Michler, and Adriaan Spierings. Mechanical anisotropy investigated in the complex slm-processed sc- and zr-modified al–mg alloy microstructure. *Advanced Engineering Materials*, 12 2018.

[24] Iso 14577-1:2015 – metallic materials – instrumented indentation test for hardness and materials parameters – part 1: Test method. Standard, International Organization for Standardization, Geneva, CH, jul 2015.

[25] David Shuman, André Costa, and Margareth Andrade. Calculating the elastic modulus from nanoindentation and microindentation reload curves. *Materials Characterization - MATER CHARACT*, 58:380–389, 04 2007.

[26] Robert A. Haynes, Ed Habtour, Todd Henry, Daniel Cole, Volker Weiss, Antonios Kontsos, and Brian Wisner. *Damage Precursor Indicator for Aluminum 7075-T6 Based on Nonlinear Dynamics*, pages 303–313. 01 2019.

[27] Ed Habtour, Daniel Cole, Christopher Kube, Todd Henry, Robert Haynes, Frank Gardea, Tomoko Sano, and Tiedo Tinga. Structural state awareness through integration of global dynamic and local material behavior. *Journal of Intelligent Material Systems and Structures*, page 1045389X1982848, 02 2019.